



**Politecnico  
di Torino**

*Master of Science in Civil Engineering*

*Master degree's thesis*

**Fatigue characterization of bituminous binders**

**Supervisors: Professor Ezio SANTAGATA**

**Co-supervisor: Sadegh YEGANEH**

**Candidate: Ozge ULKER (S289597)**

October 2023

## **Acknowledgment**

I wish to convey my profound appreciation to all the professors who provided assistance to me during my academic career.

Second, I want to thank my master responsible for allowing me to take part in such a top-notch master's program.

I want to express my sincere gratitude for the wonderful experience I had in my academic career. I'm appreciative for getting this experience and getting started in my career in such a positive and supportive environment.

My master's thesis supervisor, Prof. Ezio Santagata, has my undying gratitude for his aspirational leadership, incredibly insightful conversations, and genuinely warm counsel.

I want to extend my sincere gratitude to Sadegh Yeganeh, the co-supervisor of my master's thesis, for his guidance and support.

My colleagues, families, and siblings are sources of inspiration and motivation. I appreciate their help and encouragement in helping me achieve my goals.

## Abstract

Bituminous binder is a fundamental component in road construction, influencing the durability and lifespan of road surfaces. One of the important distresses in bituminous asphalt mixtures is fatigue failure at intermediate temperatures. Fatigue resistant strongly related to binder properties used in the asphalt mixture. During the last decade, different tests has been defined to investigate the fatigue resistance of binder. Traditionally, time sweep test was used to analyze fatigue properties of binders. However, time sweep challenges with the long duration of testing, the linear amplitude sweep (LAS) test is introduced and proposed by researchers as faster method to estimate the fatigue resistance of asphalt binder.

The framework of this study relies on laboratory experiments and various analysis method to investigate the fatigue characterization of different binders by use of dynamic shear rheometer (DSR). In this regard, the LAS test has been chosen as the main protocol to be employed in this research. Materials considered in this study contain two type of neat binders and two different polymer modified binders (PMB). To provide more comprehensive view, these 4 different binders have been subjected to two level of aging (short-term by RTFO and long-term by use of PAV), thus, the investigation covers 12 samples with various properties. Although the standard is required aged samples, the un-aged samples also were tested. The aging of binders expanded the variety of samples and provides the ability to observe the effect of aging in fatigue resistance of binders.

This study focuses on the different failure criterions introduced for analyzing LAS test results. The performance predictive accuracy of LAS test is strongly dependent on the selected failure definition. The current standard suggested the peak of shear stress as the failure point, while the peak of pseudo strain energy (PSE) and the 35% reduction in loss shear modulus of binder are also employed as other well-known failure criterions in this research.

Result showed coherency between these three failure criterions while the 35% reduction in loss shear modulus showed overestimated results in comparison to the other two failure criterions. Moreover, analyzing results related to the peak of PSE criteria is not always applicable specially in case of testing polymer modified binders.

Overall, this study investigates the critical issue of understanding the fatigue properties of bituminous binders to improve road infrastructure sustainability.

## Sommario

Il legante bituminoso è un componente fondamentale nella costruzione stradale, influenzando la durabilità e la durata delle superfici stradali. Uno dei problemi più importanti nelle miscele di asfalto bituminoso è la rottura per fatica a temperature intermedie. Resistenza alla fatica fortemente correlata alle proprietà del legante utilizzato nella miscela di asfalto. Nell'ultimo decennio sono stati definiti diversi test per indagare la resistenza a fatica del legante. Tradizionalmente, il test time-sweep veniva utilizzato per analizzare le proprietà di fatica dei leganti. Tuttavia, a causa della lunga durata dei test, il test di scansione in ampiezza lineare (LAS) viene introdotto e proposto dai ricercatori come metodo più rapido per stimare la resistenza alla fatica del legante asfaltico.

La struttura di questo studio si basa su esperimenti di laboratorio e vari metodi di analisi per studiare la caratterizzazione della fatica di diversi leganti mediante l'uso del reometro a taglio dinamico (DSR). A questo proposito, il test LAS è stato scelto come protocollo principale da impiegare in questa ricerca. I materiali considerati in questo studio contengono due tipi di leganti puri e due diversi leganti modificati con polimero (PMB). Per fornire una visione più completa, questi 4 diversi leganti sono stati sottoposti a due livelli di invecchiamento (a breve termine mediante RTFO e a lungo termine mediante l'uso di PAV), pertanto l'indagine copre 12 campioni con varie proprietà. Sebbene lo standard richieda campioni invecchiati, sono stati testati anche i campioni non invecchiati. L'invecchiamento dei leganti ha ampliato la varietà di campioni e offre la possibilità di osservare l'effetto dell'invecchiamento sulla resistenza alla fatica dei leganti.

Questo studio si concentra sui diversi criteri di fallimento introdotti per analizzare i risultati dei test LAS. L'accuratezza predittiva delle prestazioni del test LAS dipende fortemente dalla definizione di guasto selezionata. Lo standard attuale suggerisce il picco dello sforzo di taglio come punto di rottura, mentre il picco dell'energia di pseudo deformazione (PSE) e la riduzione del 35% del modulo di perdita di taglio del legante sono utilizzati anche come altri criteri di rottura ben noti in questa ricerca.

Il risultato ha mostrato coerenza tra questi tre criteri di fallimento mentre la riduzione del 35% del modulo di taglio delle perdite ha mostrato risultati sovrastimati rispetto agli altri due criteri

di fallimento. Inoltre, l'analisi dei risultati relativi al picco dei criteri PSE non è sempre applicabile, specialmente in caso di test di leganti modificati con polimeri.

Nel complesso, questo studio indaga la questione critica della comprensione delle proprietà di fatica dei leganti bituminosi per migliorare la sostenibilità delle infrastrutture stradali.

# Table of Contents

Acknowledgment .....	1
Abstract .....	2
Sommario .....	3
List of Figures .....	7
List of Tables .....	8
List of Equations .....	9
List of Acronyms .....	9
Chapter 1: INTRODUCTION.....	11
1.1 Introduction.....	12
1.2 State of Art.....	13
1.3 Objectives .....	18
Chapter 2: MATERIALS and METHODS.....	19
2.1 Introduction.....	21
2.2 Material Selection .....	21
2.3 Aging of Bitumen .....	22
2.3.1 Rolling Thin Film Oven Test (RTFOT).....	22
2.3.2 Pressure Aging Vessel (PAV).....	25
2.4 Dynamic Shear Rheometer (DSR).....	28
2.5 Simplified Viscoelastic Continuum Damage (S-VECD) Model .....	31
2.6 Analytical Methods .....	32
2.6.1 Dissipated Energy-Based Analytical Method.....	32
2.6.2 Pseudo Strain Energy-Based Analytical Method.....	35
2.7 Fatigue Failure Criteria .....	39
2.7.1 Failure criterion based on %35 Reduction in Loss Modulus.....	39
2.7.2 Failure criterion base on Max Shear Stress.....	42
2.7.3 Failure criterion based on Max Pseudo Strain Energy (PSE).....	44
Chapter 3: EXPERIMENTAL PLAN.....	46
3.1 Introduction.....	47
3.2 Setting of the test and specimen preparation .....	47
3.3 Evaluation of the fatigue properties using data from Standard.....	50
3.4 Calculation of Fatigue Life Parameters .....	50

Chapter 4: RESULTS and DISCUSSIONS .....	52
4.1 Introduction.....	53
4.2 Fatigue Line Parameters .....	54
4.3 Comparison of Fatigue resistance at different aging level.....	58
4.3.1 Analysis based on %35 Reduction in $ G^*  \cdot \sin \delta$ Failure Criteria.....	58
4.3.2 Analysis based on Maximum Shear Stress Failure Criteria.....	59
4.3.3 Analysis based on Pseudo Strain Energy Failure Criteria .....	61
4.4 Comparison of Different Failure Criterions.....	62
4.5 Comparison of binder type.....	67
4.6 Comparison on different scenarios .....	71
Chapter 5: CONCLUSIONS.....	76
References.....	79

## List of Figures

Figure 1 Selected materials from different refineries and sources. ....	22
Figure 2 Placed Rolling Thin Film Oven Test containers onto the rotating platform. ....	23
Figure 3 RTFOT jars. The bottle at left is after, middle, before the test. ....	24
Figure 4 Pressure Aging Vessel. ....	25
Figure 5 Pour of RTFO binder into the pan. ....	27
Figure 6 Sinusoidal stress and phase angle. ....	29
Figure 7 A schematic representation of the Physica MCR 302 rheometer [35]. ....	30
Figure 8 S-VECD Model parameters. ....	31
Figure 9 The diagram shows the PSE released and stored during the LAS test. ....	38
Figure 10 Simulation of %35 Reduction in $G^*$ failure criteria. ....	39
Figure 11 Example of $ G^*  \cdot \sin \delta$ vs Damage Plot with Curve-Fitting. ....	41
Figure 12 Normalized $N_f$ to 1 million ESALs versus the applied shear strain. ....	42
Figure 13 The maximum Shear stress-based failure criterion simulation. ....	42
Figure 14 Plotting the $ G^*  \cdot \sin \delta$ against the damage, along with a curve fit. ....	43
Figure 15 Example of damage model adopted on PSE S-VECD model. ....	45
Figure 16 Dynamic shear rheometer (MCR302) ....	48
Figure 17 Tested binder preparation first step ....	48
Figure 18 Sample after the test ....	49
Figure 19 Adhesion problem ....	49
Figure 20 Trimming of the sample ....	49
Figure 21 Rheplus software interfaces. ....	50
Figure 22 Resulted from %35 reduction in $ G^*  \cdot \sin \delta$ failure criteria. ....	59
Figure 23 Resulted from max shear strain failure criteria. ....	60
Figure 24 Resulted from pseudo strain energy failure criteria. ....	61
Figure 25 Resulted from using different failure criteria (Sample A). ....	63
Figure 26 Resulted from using different failure criteria (Sample B). ....	64
Figure 27 Resulted from using different failure criteria (Sample C). ....	65
Figure 28 Resulted from using different failure criteria (Sample D). ....	66
Figure 29 Resulted from unaged samples using all failure criteria. ....	68
Figure 30 Resulted from long-term aged samples using all failure criteria. ....	69
Figure 31 Resulted from short-term aged samples using all failure criteria. ....	70
Figure 32 Resulted from unaged binder B using PSE failure criteria. ....	71
Figure 33 Resulted from unaged binder D using PSE failure criteria. ....	72

## List of Tables

Table 1 The Selected Asphalts binders.....	21
Table 2 The average value of parameters A&B versus $N_f$ (A sample).....	55
Table 3 The average value of parameters A&B versus $N_f$ (B sample).....	55
Table 4 The average value of parameters A&B versus $N_f$ (C sample).....	56
Table 5 The average value of parameters A&B versus $N_f$ (D sample).....	57
Table 6 Summary parameter obtained from LAS-PSE failure criterion.....	74
Table 7 Summary parameter obtained from LAS- $\tau_{max}$ failure criterion.....	74
Table 8 Summary parameter obtained from LAS- %35 reduction in $ G^*  \cdot \sin \delta$ failure criterion.....	74

## List of Equations

## List of Acronyms

---

<b>Acronym</b>	<b>Definition</b>
AASHTO	American Association of State Highway and Transportation Officials
DCC	Damage characteristic curve
DE	Dissipated Energy
DSR	Dynamic Shear Rheometer
LAS	Linear Amplitude Sweep
PAV	Pressure Aging Vessel
PMB	Polymer Modified Binder
PSE	Pseudo Strain Energy
RTFO	Rolling Thin Film Oven
S-VECD	Simplified Viscoelastic Continuum Damage
SUPERPAVE	Superior Performance Pavements
VECD	Viscoelastic Continuum Damage



## **Chapter 1:**

# **INTRODUCTION**

## 1.1 Introduction

Civil engineering is a constantly evolving field, marked by significant advancements that often lead to new discoveries and new criteria. One of the foremost challenges facing civil engineers today is the development of innovative approaches to enhance asphalt pavement performance, optimize productivity, and promote the sustainability of crucial road infrastructure projects. This challenge is particularly important because bituminous binders are a key component in road construction, and their effectiveness can have a significant impact on the quality and durability of road infrastructure.

Bituminous binders are highly susceptible to fatigue cracking, which poses a significant challenge for pavement engineering. This type of damage occurs due to repeated traffic loading, leading to weakened and cracked asphalt binder and eventual pavement failure. The implications of this damage are extensive, including a negative impact on driving comfort and overall pavement performance during its long-term service life [1]. Well-designed asphalt mixes with a fatigue-resistant binder have been demonstrated to offer a superior performance over time compared to mixes with a binder that is susceptible to fatigue [2].

Fatigue cracking is a multifaceted phenomenon, influenced by various factors including the type and properties of the asphalt binder, composition of the asphalt mixture, traffic loading, and environmental conditions [3]. Accurately assessing and predicting fatigue performance of asphalt binders is essential to establish dependable methods for predicting their performance in different scenarios.

A range of fatigue performance tests have been developed to evaluate the ability of asphalt binders and mixtures to endure repeated loads over time. Such tests are crucial for characterizing the fatigue properties of these materials and provide valuable insights into the underlying causes of fatigue failure. Among the tests that have been suggested, the time sweep (TS) and linear amplitude sweep (LAS) tests have emerged as noteworthy options for enhancing the characterization of asphalt binders. Although the traditional TS test is reliable for estimating fatigue failure, it is time-consuming. LAS has been shown to overcome the limitations of TS tests [4].

A significant amount of research has been conducted to develop fatigue failure definitions and criteria for asphalt materials. The present study endeavors to conduct a comparative analysis

of common failure criteria for the fatigue testing of asphalt binders. The main objective is to identify a suitable fatigue failure criterion and an analytical method for the assessment of asphalt binders through the LAS test. The findings of this study will contribute to the development of more robust and reliable fatigue failure criteria and testing methods for asphalt binders. This, in turn, will enhance the accuracy and effectiveness of pavement design and improve the overall performance and sustainability of asphalt pavements.

## **1.2 State of Art**

In previous research, several studies have explored the influence of binder aging on fatigue performance, advancing the development of high-performance binders using various modification techniques. However, characterizing the fatigue properties of high-performance binders requires more extensive investigation, particularly by comparing different analytical methodologies. In the following section, present an comprehensive overview of literature review discussed,

The current research community has invested significant efforts into comprehending and characterizing the fatigue cracking resistance of asphalt binder. Despite the progress made, there still exists a notable disparity between laboratory tests and the actual fatigue resistance of a given binder. This discrepancy has highlighted the need for further research and development in the field of asphalt binder fatigue cracking resistance [5]. It is crucial to bridge the gap between laboratory results and real-world performance to provide reliable and accurate data for binder selection and pavement design.

Starting with discussion on fatigue cracking, which originates from the bottom of the asphalt layer in flexible pavements, is a primary source of pavement distress and reduces the service life of the pavement. In the phenomenon of bottom-up cracking, which is caused by tensile strain in the asphalt layer, the role of the asphalt binder is prominent [6]. It is essential to understand this mechanism to ensure that the pavement is designed and maintained correctly, thereby prolonging its lifespan. A focus on the asphalt binder's role in this cracking phenomenon paves the way for the development of more effective strategies to mitigate this issue and enhance the durability of flexible pavements. Fatigue cracking in asphalt concrete typically initiates and propagates within the binder phase, which is generally considered to be the weakest component of the material. Moreover, the process of aging experienced by asphalt

pavement during both construction and usage also exerts a significant influence on the fatigue resistance demonstrated by the asphalt binders. Consequently, the examination of the fatigue resistance of aged asphalt binders is of paramount importance for the design, construction, and maintenance phase of asphalt pavements, particularly for the pavements [7]. The findings of such investigations hold immense value, offering insights that can inform the development of effective strategies for enhancing the longevity and durability of asphalt pavements.

The development of binder tests to understand binder fatigue properties has been a focus of significant research efforts. In the earliest studies, The Time Sweep test is a method used to test the durability of asphalt binders. The test involves repeatedly loading a sample of the material with a Dynamic Shear Rheometer (DSR) until it reaches a specific stiffness level or other criteria. The test is widely used in academic and industrial settings and is an effective tool for assessing the fatigue behavior of asphalt binders [8]. The Time Sweep test has been demonstrated as a reliable method to assess fatigue resistance in asphalt binders and has become a traditional method. However, a significant limitation of the Time Sweep test is its time-consuming nature, which challenges its adoption as a standardized testing method. In fact, The Time Sweep test involves subjecting an asphalt binder to continuous cyclic loading at a constant shear strain until fatigue failure occurs. For this reason, it is possible that the process could take multiple hours or even extend up to a few days, depending on the binder [9].

To overcome these shortcomings, researchers have been looking into alternative methods, for instance the Linear Amplitude Sweep test, for measuring the fatigue resistance of asphalt binders. Based on the LAS test methodologies, it is designed to demonstrate greater effectiveness in terms of testing duration as compared to the Time Sweep test. The LAS test involves subjecting the binder to a range of shear strain amplitudes at a consistent frequency while at the same time analyzing the response at each amplitude [10]. This provides a faster testing duration of the binder's performance in different critical scenarios. In order to decrease test timing, the duration of TS tests for specification development was entirely dependent on the applied loading amplitude [11]. To overcome this limitation the original LAS, strain amplitude loading pattern presented by Johnson was designed stepwise. However, Hintz et al. later simplified it to a linear strain amplitude sweep spanning from 0.1 to 30% [12].

Furthermore, the test results from the LAS have exhibited a reasonable correlation with the data on field fatigue cracking obtained from the Long-Term Pavement Performance (LTPP). This finding indicates that LAS can serve as a reliable technique to predict the risk of fatigue cracking in pavement structures [13].

The LAS test evaluates asphalt binder performance under cyclic loading conditions by subjecting specimens to cyclic shear loading with increasing load amplitudes [14]. The process involves two steps. Initially, a frequency sweep is carried out at a fixed strain of 0.1% to ascertain the undamaged reaction of a binder sample. Subsequently, a linear oscillatory shear strain amplitude sweep is executed to gauge the sample's resistance to fatigue damage [15]. It should be emphasized that conventional rheometers are not capable of instantaneously altering loading amplitude, such as a 1% strain increase between two intervals, which is essential for the original LAS procedure.

The analysis of the LAS test results employs the principles of the Viscoelastic Continuum Damage (VECD) model. This model has been extensively used by numerous researchers to successfully characterize the fatigue performance of asphalt mixtures. The VECD model has proved to be an efficacious approach for evaluating the damage accumulation and progression in the asphalt mixtures under repeated loading. It provides a reliable framework for comprehending the complex viscoelastic behavior of asphalt mixtures, which is crucial for designing durable and long-term road pavements [16]. The uses of these model for predicting fatigue performance of asphalt binders have been impeded by several difficulties, including protracted test methods and challenges associated with analyzing results obtained from modified binders. However, these challenges were overcome through the implementation of the LAS testing approach [17]. The development of this studies followed by Hintz et al. has resulted in the development of a simplified-VECD (S-VECD) model for characterizing asphalt binder damage in shear fatigue loading on DSR. This model has the potential to revolutionize the asphalt industry by providing a more accurate and efficient method for characterizing asphalt binder damage [16].

The performance predictive accuracy of LAS test is strongly dependent on the selected failure definition. Several methods and models have been developed for calibrating the S-VECD theory to analyze LAS test results [18]. Among the different analytical analyses, there is a

significant effect on increasing the accuracy for identifying the fatigue properties of asphalt binders. Thus, it is necessary to investigate the different analytical methods for LAS test results.

Following, it is important to discuss the LAS test procedure followed by details on the common different analysis procedures used for the analysis of measured data in the LAS test. Previously, the phenomenological model was the most commonly used and classical model to predict fatigue life. This model establishes a correlation between fatigue life and the initial strain or stress level. The fatigue failure criteria in this model is typically associated with a 50 percent reduction in the initial stiffness or complete fracture of the specimen. The model has certain limitations that need to be taken into consideration. Firstly, it does not consider damage evolution which means that it can only be applied to a specific set of loading conditions. Secondly, the fatigue relationship derived from this model is dependent on various factors such as material type, mode of loading (controlled stress or strain), loading conditions, and test method (four-point bending beam, two-point cantilever, etc.). Furthermore, the model is not suitable for investigating fatigue endurance limit concept and healing phenomenon at low strain/damage levels. To improve this outcome the dissipated energy approach has been introduced for fatigue analysis [19]. Dissipated energy approaches offer a more effective alternative to the arbitrary 50% loss in initial stiffness criterion, as they are grounded in mechanistic principles and are sensitive to material variations. Furthermore, fracture mechanics-based indices have demonstrated their usefulness in the analysis of asphalt materials [13]. The dissipated energy concept is a key factor in the development of surrogate models for predicting fatigue life which describes the energy that is lost during each loading cycle. This measurement captures the effects of both the imposed strain and the dynamic mixture properties [19].

Over the past decade, a novel method for assessing the failure of asphalt mixtures in fatigue testing has been developed, which is based on the concept of Pseudo-Strain Energy (PSE). This approach has been further extended to the LAS test for assessing the performance of asphalt binders [20]. The stored PSE is a key determinant in identifying the failure point during the Linear Amplitude Sweep (LAS) test conducted on asphalt binders. Analysis of the results indicates that the proposed failure criterion, which corresponds to the maximum stored PSE, is dependent on the material. Importantly, a unique relationship exists between the average

release rate of PSE ( $G^R$ ) and fatigue life ( $N_f$ ), which is independent of loading history and temperature [21].

The development of fatigue analysis method is an ongoing process, with new criteria being introduced. It is important to conduct a comprehensive comparison of these criteria to provide guidance for future investigations, with the goal of enhancing our comprehension of the complicated processes underlying fatigue failure. Furthermore, such a comparison can help in the development of more precise and reliable methods for forecasting fatigue life, as well as the design of components and structures that show greater resistance to fatigue.

The accurate definition of failure in the LAS test is crucial in determining the appropriate analysis method. This section briefly presents a literature overview of the principles and latest protocols for this common criterion.

Earliest, the AASHTO TP 101-12 [22] standard defines failure of asphalt mixture as a 35% reduction in undamaged  $G^* \cdot \sin \delta$ . This criterion conforms to the traditional fatigue failure criterion of asphalt mixture, which is a 50% reduction in initial stiffness. However, it is noteworthy that this criterion is based on an arbitrary selection and lacks both theoretical and phenomenological justification [23]. Nowadays, this older provisional standard replaced by final in AASHTO T 391-20; two procedures utilizing viscoelastic continuum damage theory were conducted to determine the fatigue life criterion and the nondamaged material parameter ( $\alpha$ ) in accordance with the established standard. The first procedure entailed a frequency sweep test by applying constant amplitude oscillatory shear loading at various frequencies. The second procedure utilized oscillatory shear in strain-control mode at a frequency at 10 Hz using amplitude sweep testing [24].

There is another common failure criterion which is the Maximum Stress Criterion, introduced by AASHTO TP101-14 [25], is a commonly used failure criterion that determines the number of cycles to failure. Failure occurs when the shear stress versus shear strain curve reaches a peak. As regards, Fatigue failure causes a significant change in material integrity, reducing the required shear stress to increase shear strain [23].

The pseudo strain energy failure criterion is a also widely-used method to determine failure in materials. It is principles by measuring the amount of stored PSE against the number of cycles.

When a peak in the stored PSE is reached, it means that the material can no longer store any more energy as the strain increases [26].

Briefly, understanding the fatigue behavior of asphalt binders is critical for improving road infrastructure sustainability. This is especially significant when considering diverse aging conditions and incorporating both neat and polymer-modified binders. While the Time Sweep test has been traditionally used to analyze fatigue properties of binders, the LAS test has been proposed as a faster and reliable alternative. However, selecting the appropriate failure criteria is important for accurate results. This study provides valuable insights into different failure criteria and their applicability for different types of binders under various scenarios. Overall, both methods have their limitations, and further research is needed to improve the accuracy and efficiency of fatigue testing for asphalt binders.

### **1.3 Objectives**

Within the framework of this research, the primary objective is to develop a comprehensive evaluation that includes two distinct methods for analyzing fatigue and three different approaches for determining fatigue failure criteria. The methodologies will be thoroughly examined in the specific context of linear amplitude sweep (LAS) tests, which are essential in road infrastructure applications.

The primary focus of this study pertains to evaluating the efficacy of these analytical methodologies in the context of characterizing high-performance asphalt binders. To achieve the main goal, the binders that have been chosen, specifically chosen from different sources and origins characteristic, will undergo a rigorous assessment across various scenarios. The presented scenarios encompass different levels of binder aging, the implementation of specific failure criteria, and the crucial examination of binder selection.

## **Chapter 2:**

# **MATERIALS & METHODS**



## 2.1 Introduction

This chapter has the aim of explaining the research project and illustrate all the test used, pointing out the purpose, the specifications, and theory on the background. In this chapter, after a short explanation about the materials, the aging process has been explained. Then after, the equipment used are introduced. The final part of this chapter is dedicated to discussing about the analysis methods and different failure criterions.

## 2.2 Material Selection

In this section, a comprehensive examination is presented regarding the thoroughness of the process used during the selection of the materials that form the fundamental basis of academic research. Selecting the right materials for this study is extremely important. The reliability and accuracy of the findings are directly affected by this. These binders were sourced from different refineries and geographical origins, illustrating the inherent diversity in asphalt materials throughout regions. The wide range of options available for binder selection is consistent with our overarching goal of presenting an extensive understanding of asphalt binder performance. The list of asphalt binders used in this study are presented in Table 1.

<b>Code</b>	<b>Sample ID</b>	<b>Asphalt Types</b>
<b>A</b>	626	NEAT
<b>B</b>	470	PMB
<b>C</b>	275	NEAT
<b>D</b>	488	PMB

*Table 1 The Selected Asphalts binders.*

This study analyzes the effects of aging on four different binders through two levels of aging: short-term aging using the Rolling Thin Film Oven and long-term aging using the Pressure Aging Vessel. As a result, the investigation consists of a total of 12 samples, each with distinct characteristics.



*Figure 1 Selected materials from different refineries and sources.*

## **2.3 Aging of Bitumen**

In order to investigate the properties of both unaged, short-term aged and long-term aged binders, samples were subjected to aging simulations following standards.

### **2.3.1 Rolling Thin Film Oven Test (RTFOT)**

The Rolling Thin-Film Oven Test (RTFOT) has been used to simulate the short-term aging of asphalt binder, an essential procedure for analyzing and forecasting the performance and deterioration of pavements during their early stages. The aging of the asphalt binder during manufacturing and installation causes this phenomenon. The Superior performance pavements (Superpave) performance grade (PG) binder specification needs the evaluation of short-term aged bitumen at higher temperatures to assess its fatigue and rutting resistance. This requirement aligns with the fundamental principle of testing binders under conditions that closely reproduce real-world performance.

The adoption of standards, particularly the RTFOT, is regulated by established protocols, which include AASHTO T 240 and ATSM D 2872, which specifically address the impact of heat and air on an asphalt film in motion (also referred to as the Rolling Thin-Film Oven Test, or RTFO). Also, rigorous adherence to the British Standard EN12607-1:2007 guidelines was strictly adhered to throughout the implementation of this test, leading to a calibrated reduction in the duration of the test from 85 to 75 minutes. [27]

In order to prepare for the RTFO test, it is crucial to subject an asphalt binder sample to sufficient heating until it reaches an appropriate degree of fluidity, facilitating a smooth pouring

process. [6] Following that, the sample is agitated to achieve uniformity and eliminate any trapped air bubbles. Out of the total of eight jars, two are specifically identified as the "mass change" bottles, as they are labeled and weighed when empty. The prescribed standard indicates that a maximum of 30 grams of asphalt should be poured into each jar to prevent any drainage of the binder from the bottles during the test while also ensuring the formation of a thin film of binder on the bottle's surface. The bottles undergoing the process of "mass change" are subsequently permitted to reach ambient temperature within desiccators for a duration of 60 minutes. Following this, their mass is measured and documented as  $M_1$  and  $M_1'$ .



*Figure 2 Placed Rolling Thin Film Oven Test containers onto the rotating platform.*

The bottles are positioned within the carousel on the RTFOT equipment, which is subsequently activated.

For optimal test conditions, it is suggested that the oven temperature reach the designated temperature of  $163^{\circ}\text{C}$  within a duration of 15 minutes subsequent to the placement of the RTFOT jars in the carousel. Therefore, it is advisable to preheat the oven for a duration of at least 30 minutes before commencing the experiment. The duration of the Rolling Thin Film Oven Test (RTFOT) is 75 minutes, starting when the temperature reaches a stable point of  $163^{\circ}\text{C}$ . During this time frame, the asphalt binder samples are subjected to a continuous rotation on a carousel, which guarantees a uniform and consistent exposure to both heat and

airflow. This process occurs at a rate of 4000 ml/min, thereby facilitating comprehensive mixing and evaluation of the samples.

Following a 55-minute cooling period, the two bottles containing the masses of interest are reweighed, resulting in recorded masses denoted as  $M_2$  and  $M_2'$ . The remaining residue is subsequently discarded. The samples are subsequently maintained for utilization in DSR equipment tests or for the purpose of PAV-aging. The calculation for determining the percentage change in mass of a sample relative to its initial mass is expressed as:

$$100 * \left( \frac{M_2 - M_1}{M_1 - M_0} \right)$$

*Equation 1*

In which:

$M_2, M_2'$  : The combined mass of the glass container and the sample after to the testing procedure.

$M_1, M_1'$  : The combined weight of the glass containers and the sample after it has been cooled.

$M_0, M_0'$  : The mass of the glass containers is measured to the nearest 1 mg.



*Figure 3 RTFOT jars. The bottle at left is after, middle, before the test.*

### 2.3.2 Pressure Aging Vessel (PAV)

Pressure Aging Vessels (PAVs) are used to simulate long-term oxidative aging of asphalt binders by exposing them to pressurized, heated air. The observed aging condition in asphalt binders from seven to ten years exhibits similarities to this specific aging process [28]. The Superpave PG binder specification requires the evaluation of fatigue and reduced temperature cracking resistance of long-term aged asphalt binders through testing at intermediate and cold temperatures.



*Figure 4 Pressure Aging Vessel.*

Hence, it is important to simulate the aging of asphalt binder to forecast distress.

This response aims to present a concise overview of the esteemed Pressure Aging Vessel (PAV) technique, as documented in the authoritative AASHTO R 28 standard [29]. This particular method serves as a crucial component in the field of asphalt binder aging evaluations.

Asphalt aging involves a complex interplay of multiple factors, with oxidation emerging as a prominent contributor. Over time, this persistent procedure imparts an escalating viscosity to bitumen, propelling it toward the brink of metamorphosis [30]. However, at a particular stage in this chemical process, the asphalt acquires the ability to overcome oxidation, leading to its permanent immobilization of highly reactive elemental constituents.

According to Bahia and Anderson's 1995 study, oxidation in pavement materials can occur in two distinct phases over a pavement's lifespan [31]. The dual-stage perspective on oxidation highlights the significance of taking proactive measures to mitigate binder aging throughout the entire lifespan of pavement, starting from its initial construction and extending to its ongoing use. These measures are crucial for maintaining the longevity and effectiveness of our road networks in light of this enduring challenge. These two distinct stages are:

1. During the process of mixing and laying, the increased temperature causes the asphalt binder to undergo rapid aging due to volatilization, while the extensive contact between the binder and the heated aggregate results in oxidation. During this stage, the primary mechanism of aging is the degradation of volatile components due to increased temperatures during mixing and placement. Therefore, the examination of this phase is conducted using the RTFO test.
2. Throughout the lifespan of a pavement that is actively being used, the asphalt binder component undergoes a gradual aging process as it is exposed to oxygen from the surrounding environment. This exposure leads to chemical reactions taking place within the pavement.

The initial consideration for developing a procedure to simulate long-term aging through oxidation involved the use of oven tests. Thin bitumen films were heated to speed up the oxidation process. Nevertheless, this approach proved to be unsuitable, as the samples exhibited a considerable loss of volatile components. It is important to note that this observation was not corroborated by field tests conducted on older pavements currently in use. Consequently, the employed methodology involves the application of elevated pressure, which serves to enhance the rate of oxygen diffusion into the asphalt binder specimen while simultaneously mitigating the volatiles' dissipation. In addition, the process of aging can be conducted without the requirement of elevated temperatures, and it is possible to approximate the prevailing field climate conditions.

The PAV process is usually accomplished for 20 hours at either 90, 100, or 110°C, depending on the climate to be simulated. These details were chosen for practical rather than theoretical reasons. The PAV time of 20 hours allows for one test plus the removal of completed samples and insertion of new samples within one day [32].

The phases of the PAV procedures are outlined as follows:

1. The short-term aged asphalt binder known as RTFO is subjected to heating until it reaches a sufficiently fluid state for pouring, followed by agitation. The preheated thin-film oven pans are filled with 50 grams each and subsequently inserted into a pan holder. This panholder is then positioned within the preheated PAV.

2. The PAV specimen is hermetically sealed and subsequently permitted to revert to the ambient temperature.
3. After the desired temperature is achieved, the PAV is pressurized to a level of 2.07 MPa, and this pressure is sustained for a duration of 20 hours.
4. Upon reaching the conclusion of the aging process, the pressure is systematically alleviated, and the pans are cautiously extracted from the PAV.
5. The pans are subsequently introduced into an oven and subjected to a temperature of approximately 163°C for a duration of approximately 15 minutes. This step is undertaken with the purpose of preparing the asphalt-aged binder for subsequent testing procedures.
6. Following the aforementioned heating process, the specimen is subsequently introduced into a vacuum oven for a duration of 30 minutes in order to eliminate any residual gases. The implementation of this procedure is imperative in order to eliminate any trapped air that could potentially compromise the precision and dependability of subsequent tests.

The PAV-aged binder has been prepared and is now available for subsequent testing. Specifically, it has been utilized for examinations of the DSR.



*Figure 5 Pour of RTFO binder into the pan.*

## 2.4 Dynamic Shear Rheometer (DSR)

It is the basis for the study of the rheology of bitumen, especially at intermediate and high service temperatures. The sample is subjected to a sinusoidal form stress. The system provides various rheological parameters, including the phase angle and complex modulus, as well as the rutting parameter. The raw data can be plotted and elaborated in many ways as we will further see.

To achieve the objectives of this research investigation, the dynamic shear rheometer (DSR) has been selected as the instrument of choice for evaluating the viscous and elastic properties exhibited by a bitumen sample after performing thermal conditioning. The characterization of the sample is accomplished by subjecting it to different stress or strain regimens, and the understanding of these regimens is obtained from analyzing the resulting deformation response and stress data. The measurements take place across a range of temperatures, levels of strain and stress, and frequencies of testing, thereby including an extensive dataset. The DSR software is capable of automatically executing the required calculations. The software employs the subsequent formulas [33]:

$$\tau_{max} = \left( \frac{2M}{\pi r^3} \right)$$

*Equation 2*

which:

$\tau_{max}$ : Applied maximum stress

M: Torque

r : parallel disks diameter

$$\gamma_{max} = \frac{\theta * r}{h}$$

*Equation 3*

Where:

$\gamma_{max}$  : shear strain

h : gap between parallel disks

$\theta$  : deflection angle

The shear stress and strain in equations 2 and 3 are contingent on the radius of the parallel disks and exhibit varying magnitudes from the center to the perimeter of the disk. The calculation of shear stress, shear strain, and complex modulus  $G^*$  involves determining their values at the maximum radius, which is a function of the radius raised to the fourth power. The instrument accurately measures the phase angle, denoted as  $\delta$ , by precisely determining the sinusoidal waveforms of both the strain and torque.

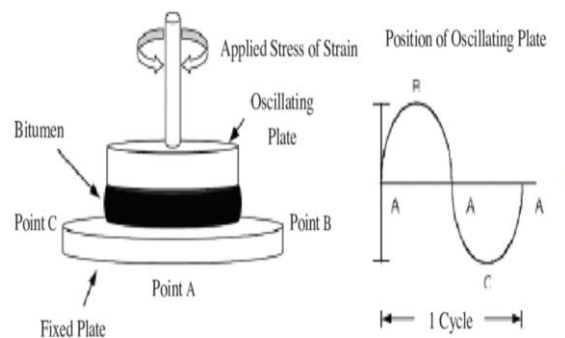


Figure 6 Sinusoidal stress and phase angle

Two different paradigms, namely the controlled-strain technique and the controlled stress method, can be used for performing testing operations. It is important to highlight that data obtained from both paradigms can be easily exchanged, which enhances the overall comprehensibility of the gathered information. The controlled-strain methodology involves subjecting the test specimen to a sinusoidal strain pattern while simultaneously measuring the appropriate magnitude and phase of the resulting stress. The determination of strain value is strongly linked with the value of the complex modulus, which is an essential parameter that improves the understanding of the material's behavior under different conditions [34].

On the other hand, the controlled-stress method involves the application of a stress wave form that exhibits sinusoidal characteristics. Meanwhile, it analyzes the amplitude and phase of the subsequent strain presentations. Additionally, the stress level can be ascertained using the complex modulus.

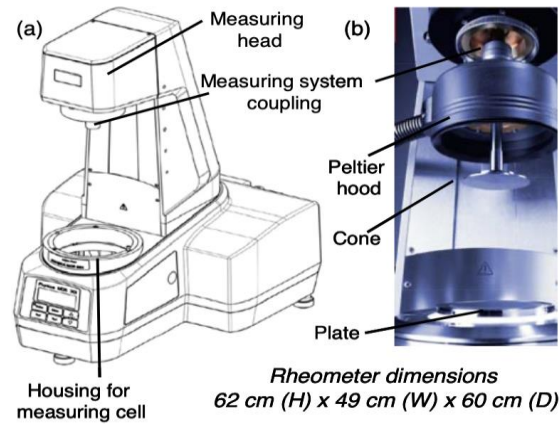


Figure 7 A schematic representation of the Physica MCR 302 rheometer [35].

The DSR naming convention may need to be revised. Dynamic forces are not taken into account in this study. The term "dynamic" pertains explicitly to how both the stresses strains are applied to the test specimen. Indeed, the Dynamic Shear Rheometer (DSR) has the potential to be employed for the purpose of viscosity measurement, as well as for conducting tests that involve the evaluation of stiffness and other viscoelastic properties of the samples. Viscosity measurements, specifically through rotational tests or creep tests, serve as valuable methods for assessing the long-term load behavior of binders. The latter tests are called dynamic tests due to applying stress/strain in an oscillatory manner. This approach enables a significant expansion of the material characterization scope while substantially reducing the testing process's duration. Indeed, the experiments conducted at a specific frequency  $\omega$  exhibit qualitative similarity to the outcomes obtained during a testing duration [36].

$$\tau = 1/\omega$$

Equation 4

The DSR comprises three primary components: the rheometer itself, the controller, and the computer. The rheometer typically consists of a housing or frame, a motor to apply strain or stress to the specimen, a transducer to measure the specimen's response, and a temperature control and measurement system. The controller is an intermediary between the rheometer and the computer, facilitating data transmission. It encompasses the necessary hardware for data acquisition and signal conditioning, specifically designed for the motors and transducers in the rheometer. The rheometer is typically operated and programmed through a personal computer.

## 2.5 Simplified Viscoelastic Continuum Damage (S-VECD) Model

When it comes to understanding the fatigue behavior of asphalt binders and designing asphalt pavements that are more resistant to fatigue cracking, the simplified Viscoelastic Continuum Damage (S-VECD) model is a valuable tool for designing them.

By using the VECD theory, it is possible to predict how a material will perform in a wide range of other situations based on the findings from only one experiment. The model's capacity to generalize the effects of a given set of variables makes this possible [12].

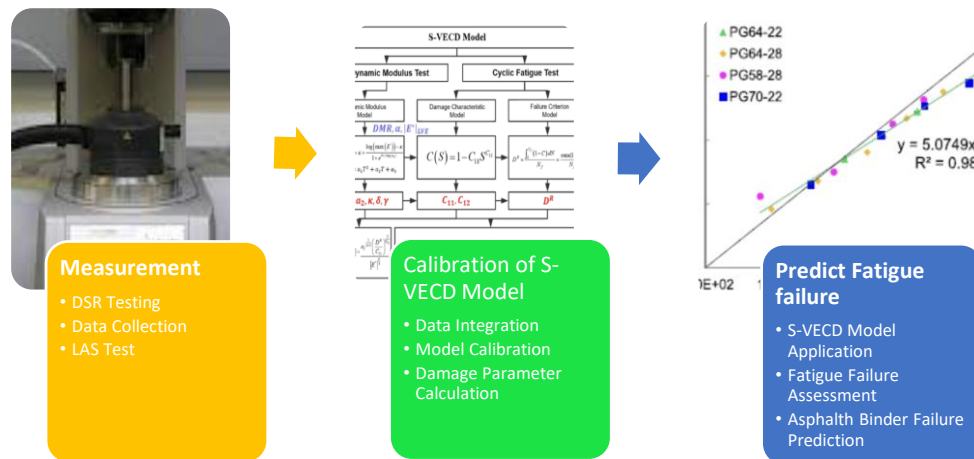


Figure 8 S-VECD Model parameters.

The most critical part of using VECD theory to characterize the fatigue resistance of asphalt materials is to establish the damage characteristic curve (DCC), which is a function of material integrity (C) and damage intensity (D). The DCC specifies the path of materials losing structural integrity caused by the damage accumulation under cyclic loading. In addition, this relationship is unique because it is independent of the test conditions (e.g., temperature, loading level, frequency, and control mode) [37]. These advantages make VECD theory widely used in fatigue damage analysis of asphalt materials.

The S-VECD model consists of four main components:

1. Schapery's extended elastic-viscoelastic correspondence principle is utilized to discern the distinct influences of damage and viscoelasticity on the quantified stiffness.
2. Schapery's work focuses on potential theory as a means of simulating the impact of damage on the macroscopic constitutive behavior.
3. The notion of time-temperature superposition is utilized in the simulation of damage progression under varying temperatures.
4. One of the key considerations in estimating the impact of loading and temperature history on eventual fatigue failure is the establishment of a failure criterion.

## 2.6 Analytical Methods

In this section, the analytical methods used in the evaluation of asphalt binder fatigue resistance within the LAS test are explained. The theoretical foundation for analyzing fatigue simulation data of binders lies in Schapery's work potential theory and pseudo strain energy (PSE) evaluation. These methodologies are:

### 2.6.1 Dissipated Energy-Based Analytical Method

It is a method for estimating asphalt binders' fatigue life and damage accumulation. The principle states that fatigue damage is proportional to dissipated energy during loading cycles. This information can be used to develop new asphalt binders and pavement design guidelines that improve the fatigue resistance of asphalt pavements. Further, we will see theory on background is adopted on fatigue life and damage accumulation estimation.

The dissipated energy technique for asphalt binder on fatigue study is advanced and gives valuable insights into how materials withstand various loading cycles. This technique emphasizes energy dissipation, which describes the material's capacity to absorb and release energy under cyclic pressures and how this affects fatigue resistance. These foundations are built on the following relations. By Schapery's theoretical framework, damage is described as [38]:

$$\frac{dD}{dt} = \left( -\frac{\partial W}{\partial D} \right)^\alpha$$

*Equation 5*

where:

D: The damage variable

W: Potential energy that has been stored

$$W = \gamma^2 * \pi * \text{sen}\delta * |G^*|$$

*Equation 6*

in which:

$\gamma$ : strain where it reaches peak

$|G^*|$ : Complex modulus

Forms of both formulas can be written by substituting equation 6 into 5 with and use of numerically integration on:

In equation 5, both the numerator and the denominator on the right side of the equation can be divided to  $dt$  produce the following expression:

$$\left(\frac{dD}{dt}\right)^{1+\frac{1}{\alpha}} = -\left(\frac{\partial W}{dt}\right)$$

*Equation 7*

By inverting the equation above, obtained as follows,

$$dD = \left((- \partial W)^{\frac{\alpha}{1+\alpha}}\right) * \left((dt)^{\frac{1}{(1+\alpha)}}\right)$$

*Equation 8*

The D can be determined using the numerical integration of the formula derived from a Riemann sum. Therefore, the relationship between the magnitude of D and the passage of time can be expressed as,

$$D(t) = \sum_{i=1}^N (\pi\gamma_0^2 (|G^*|sen\delta_{i-1} - |G^*|sen\delta_i)^{\frac{\alpha}{1+\alpha}} * (t_i - t_{i-1})^{\frac{1}{1+\alpha}})$$

Equation 9

Moreover, a theoretical framework is created and adjusted to  $|G^*|sen\delta$ ,  $D(t)$  shown:

$$sen\delta * |G^*| = C_0 - C_1((D)^{C_2})$$

Equation 10

Whereas  $C_0, C_1, C_2$  represents settings of the framework. In 2020, Sukhija & Saboo introduced  $sen\delta * |G^*| = C_0 = 1$ , from normalization process. As follows [39],

By substituting Equation 10 into Equation 6, we can derive the following expression:

$$W = (\gamma_p^2 * \pi * C_0 - C_1((D)^{C_2})$$

Equation 11

When the previous equation is now differentiated regarding  $D$ , rewritten results:

$$\frac{dU}{dD} = -(\gamma_p^2 * I_D * \pi * C_2 C_1 ((D)^{C_2-1})$$

Equation 12

Now, Equations 17 with 5, it is possible to obtain,

$$\frac{dD}{dt} = (\gamma_p^2 * I_D * \pi * C_2 C_1 ((D)^{C_2-1})^\alpha$$

Equation 13

Next, the process involves restructuring the terms and integrating both sides of the equation:

$$\frac{D^k}{k} = (\gamma_p^2 * I_D * \pi * C_2 C_1)^\alpha * t$$

Equation 14

The above closed-form solutions were based on the asphalt binder's fatigue life ( $N_f$ ),

$$N_f = \left( \frac{f(D_f)^k}{k(I_D * \pi * C_2 C_1)^\alpha} * (\gamma_p^2) \right)^{-2\alpha}$$

Equation 15

Here,  $D_f$  represents us , to point of failure at damage, and k corresponds  $(1+1-C_2)^\alpha$ .

Based on the dissipated energy approach, fatigue failure points are defined by maximum shear stresses in materials, as outlined in the AASHTO TP-101. It has been postulated that the entirety of the energy is wasted solely in the form of damage caused by the applied load. However, articles have contended that a portion of the energy may be dispersed by viscoelastic damping, indicating that the total dissipated energy cannot be attributed solely to damage.

## 2.6.2 Pseudo Strain Energy-Based Analytical Method

It is based on the principle that the fatigue damage of a material is proportional to the pseudo strain energy dissipated during fatigue loading.

According to asphalt binder fatigue analysis, the "Pseudo Strain Energy-Based Analytical Method" signifies a sophisticated methodology for evaluating the material's capacity to withstand damage caused by fatigue. The approach employed in this study is based on the fundamental principle of pseudo-strain energy, which serves as a crucial metric for measuring

the dissipation of energy within the material during cyclic loading. Following, calculations applied using Eq. 1.4, with regards to PSE:

$$\frac{dD}{dt} = \left( -\frac{\partial W_s^R}{\partial D} \right)^\alpha$$

*Equation 16*

Where:

$W_s^R$ : The stored PSE

The task is conducted by the binder to minimize deformation throughout a loading cycle. A numerical illustration of this phenomenon can be expressed as:

$$W_s^R = \left( \frac{1}{2} \right) * \tau_p * \gamma_p^R$$

*Equation 17*

Then,

$$W_s^R = \left( \frac{1}{2} \right) * (C^*) * (D) * (\gamma_p^R)^2 * DMR$$

*Equation 18*

$(C^*) * (D)$ : maximum pseudo stiffness

If rewritten as the left side, one can be obtained:

$$C^* * D = \frac{\tau_p}{DMR * (\gamma_p^R)}$$

*Equation 19*

Where:

$\gamma_p^R$ : maximum pseudo strain

$\tau_p$ : maximum stress

*DMR*: Dynamic modulus ratio (initial  $|G^*|$  where strain sweep /  $|G^*|$  where freq sweep test)

$\gamma_p^R$ , derived maximum measured strain as shown:

$$\gamma_p^R = \gamma_p |G^*|_{LVE}$$

*Equation 20*

By examining equations 19 and 20, it can be observed that the value of  $C^*(D)$  within the LVE domain is equivalent to one. The value of the binder will diminish as the strain and accumulation of damage rise.

By rearranging Equation 16 and afterwards doing mathematical integration in a manner similar to Equation 9, the calculation of the damage can be determined as follows:

$$D(t) = \sum_{i=1}^N \left( \frac{DMR}{2} (\gamma_p^R)^2 (C_{i-1}^* - C_i^*) \right)^{\frac{\alpha}{1+\alpha}} * (t_i - t_{i-1})^{\frac{1}{1+\alpha}}$$

*Equation 21*

In a manner equivalent to the differential evolution dissipated energy methods, a mathematical model can represent the correlation between the material integrity  $C^*$ ,  $D$ ,

$$C^* = 1 - T_1((D)^{T_2})$$

*Equation 22*

Where:

$T_1, T_2$ : The model constants were derived through the process of fitted curves.

Afterwards, eq. 16 transformed into previous equations:

$$-\frac{\partial U_s^R}{\partial D} = \frac{1}{2} T_1 T_2 (D)^{\frac{1}{2}-1} (\gamma_P^R)^2$$

Equation 23

Subsisting on Eq. 16, mathematically obtained as

$$\frac{dD}{dt} = (\gamma_P^R)^2 * \frac{1}{2} * T_2 T_1 ((D)^{K_2-1})^\alpha$$

Equation 24

Similarly, based on the asphalt binder's fatigue life ( $N_f$ ) calculation can be rewritten:

$$N_f = \left( \frac{f * 2^\alpha (D_f)^j}{J(|G^*|_{LVE}^2 (T_1 T_2)^\alpha) * (\gamma_p^2)} \right)^{-2\alpha}$$

Equation 25

$J$ : is represents  $1 - \alpha T_2 + \alpha$

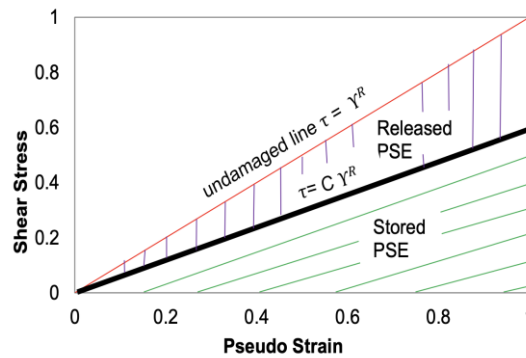


Figure 9 The diagram shows the PSE released and stored during the LAS test.

The proposed methodology, based on pseudo-strain energy, allows for the independent analysis of the viscoelastic properties of asphalt materials and the examination of damage development

separately throughout testing. Hence, the method employed for calculating the fatigue life of asphalt binders is theoretically more precise than the dissipated energy-based approach.

## 2.7 Fatigue Failure Criteria

The present conventional approach considers the peak shear stress as the point of failure, but this research additionally incorporates the peak pseudo strain energy (PSE) and the 35% decrease in the loss shear modulus of the binder as alternative and well recognized failure criteria.

### 2.7.1 Failure criterion based on %35 Reduction in Loss Modulus

The reduction of 35% in the  $|G^*| \cdot \sin \delta$  failure criterion signifies an increased vulnerability of the binder to damage under identical strain conditions. There are several potential factors that may contribute to this phenomenon, including the inclusion of modifiers, the degradation of the binder over time, the temperature at which the LAST test is performed, and the rate at which the LAS test is conducted.

The initial failure event was identified as a reduction of 35% in the magnitude of  $|G^*| \cdot \sin \delta$  (equivalent to a  $C_f$  value of 0.65 in the VECD analysis) observed during the LAS test. The identification of this reduction is significant as it enables the establishment of a more precise correlation between the prediction of  $N_f$ , which is based on LAS.

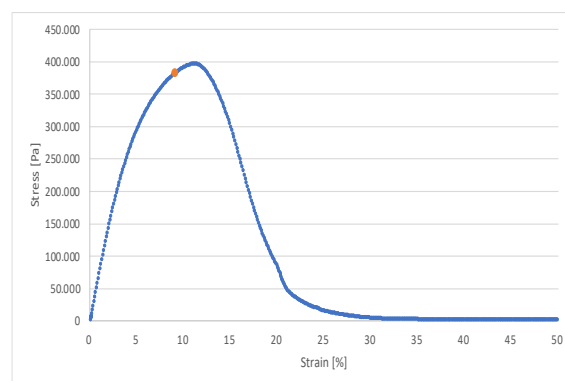


Figure 10 Simulation of %35 Reduction in  $G^*$  failure criteria.

#### 2.7.1.1 T 391-20 Standard

The AASHTO T 391-20 failure criteria is based on the assumption that a pavement failure occurs when the loss modulus of the asphalt has decreased by 35%. This protocol suggests us:

The initial stage of the analysis methodology involves the determination of the  $\alpha$  fatigue parameter, which is obtained through the execution of a frequency sweep test. The data pertaining to the dynamic modulus [ $|G^*(\omega)|$ ] and phase angle [ $\delta(\omega)$ ] at various frequencies are transformed into the storage modulus,  $G'(\omega)$ . By using the expression:

$$G'(\omega) = |G^*(\omega)| \cos \delta(\omega)$$

*Equation 26*

The storage modulus  $G'(\omega)$  is determined through the frequency sweep test, where a linear regression analysis is conducted on a logarithmic plot of  $\omega$  versus  $\log G'(\omega)$  using the given expression.

$$\log G'(\omega) = m(\log \omega) + b$$

*Equation 27*

The value of  $m$  is closely linked to the parameter  $\alpha$  that

$$\alpha = \frac{1}{m}$$

*Equation 28*

The substitution is performed in equation 9, and the summation of damage accumulation commences with the initial data point for the strain interval of one percent. The value of  $D(t)$  at each subsequent point is incrementally added to the value of  $D(t)$  from the previous point. The previously described computation is executed iteratively until reaching the ultimate data point corresponding to applying a 30% strain.

The estimation of  $C_1$  and  $C_2$  parameters can be determined based on the following relationship, where  $C_1$  corresponds to the anti-logarithm of the intercept and  $C_2$  corresponds to the anti-logarithm of the slope.

$$\log(C_0 - |G^*| \sin \delta) = \log(C_1) + C_2 \cdot \log(D)$$

*Equation 29*

Damage failure value  $D_f$  is defined as the damage that corresponds to a 35 percent reduction in undamaged  $|G^*| \cdot \sin \delta (C_0)$ , In the computation of both  $C_1$  and  $C_2$ , data points pertaining to damages below 100 are excluded from consideration, as shown:

$$D_f = (0.35) \left( \frac{C_0}{C_1} \right)^{\frac{1}{C_2}}$$

Equation 30

The binder fatigue performance can be now calculated as:

$$N_f = A_{35}(\gamma_{max})^{-\beta}$$

Equation 31

Where:

$\gamma_{max}$  : the peak expected strain

$$A_{35} = \frac{f(D_f)^k}{k(\pi I_d C_1 C_2)^\alpha}$$

Equation 32

$f$ : The loading frequency at 10 Hz

$B = 2\alpha$ ,  $k = 1 + (1 - C_2)\alpha$  taken.

The uses of the subsequent illustrative diagrams could prove to be advantageous in effectively visualizing the outcomes:

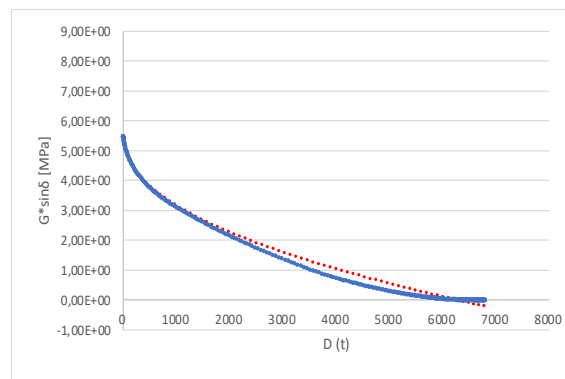


Figure 11 Example of  $|G^*| \cdot \sin \delta$  vs Damage Plot with Curve-Fitting.

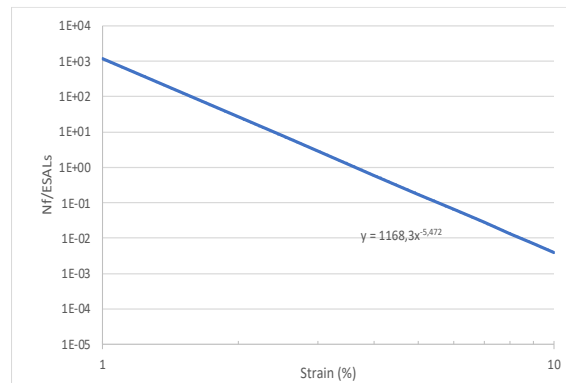


Figure 12 Normalized  $N_f$  to 1 million ESALs versus the applied shear strain.

### 2.7.2 Failure criterion base on Max Shear Stress

The maximum shear stress failure criterion is predicated upon the notion that the failure of asphalt binder occurs when the shear stress within the binder surpasses the shear strength of the binder.

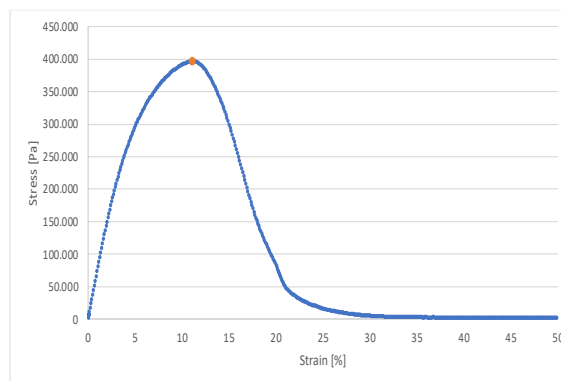


Figure 13 The maximum Shear stress-based failure criterion simulation.

The fatigue life is determined by considering the maximum stress criterion suggested by AASHTO TP101-14, wherein failure introduced once the maximum stress is reached.

#### 2.7.2.1 TP 101-14 Standard

The other standard also employs a similar analysis, although certain variations in the estimation of damages were identified, resulting in significantly divergent outcomes. Here, I will discuss highlighted point.

By remaining equation 9 which describes damage accumulation in the specimen, the initial “undamaged” value of  $|G^*|$  is the second data point, as the first point after change of material condition from rest differs from the undamaged modulus of material at the target loading frequency.

So, in this case failure at damage come up with:

$$D_f = \left( C_0 - Cat\ peak \frac{stress}{C_1} \right)^{\frac{1}{C_2}}$$

Equation 33

The calculation for the binder fatigue resistance parameter  $N_f$  is as follows:

$$N_f = A(\gamma_{max})^{-B}$$

Equation 34

Where:

$$A = \frac{f(D_f)^k}{k(\pi C_1 C_2)^\alpha}$$

Equation 35

$f$ : The loading frequency at 10 Hz

$B = 2\alpha$ ,  $k = 1 + (1 - C_2)\alpha$  taken.

The use of the following illustrative diagrams may be beneficial in effectively visualizing the results:

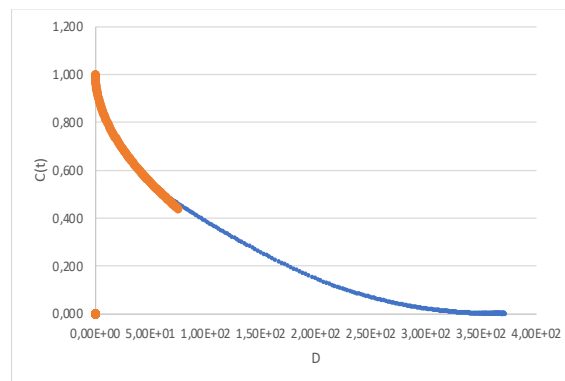


Figure 14 Plotting the  $|G^*| \cdot \sin \delta$  against the damage, along with a curve fit.

### 2.7.3 Failure criterion based on Max Pseudo Strain Energy (PSE)

Wang et al. (2015) and Sabouri and Kim (2014) have developed a failure criterion for LAS and asphalt mixtures, respectively, based on the relationship between fatigue life and the average released pseudo-strain energy until failure, denoted as GR. The stored pseudo-strain energy versus N curve is a suitable definition of failure for LAS tests, as the material loses its ability to store additional energy with the increase in strain amplitude once it fails. Similarly, a unique relationship exists between and GR for asphalt binders that is independent of the loading history. Safaei and Castorena (2015) have further demonstrated the temperature independence of the failure criterion.

GR is defined in Eq. (36)

$$G^R = \frac{W_r^R}{N_f} = \frac{A}{N_f^2}$$

Equation 36

where  $W_r^R$  is the average released pseudo-strain energy. The released pseudo-strain energy represents the difference between total pseudo-strain energy (undamaged response) and stored pseudo-strain energy (damaged response). The total pseudo-strain energy ( $W_{total}^R$ ) is determined according to Eq. (37),

$$W_{total}^R = \frac{1}{2} \tau_{p \text{ undamaged}} \cdot \gamma_p^R = \frac{1}{2} (\gamma_p^R)^2$$

Equation 37

Where  $\tau_p$  is the peak stress amplitude and  $\gamma_p^R$  is the corresponding peak pseudo-strain amplitude. Given the definition of stored pseudo-strain energy, the released pseudo-strain energy is calculated using Eq. (38), where  $C^*$  is the damage constant.

$$W_r^R = W_{total}^R - W_s^R = \frac{1}{2} (10 - C^*) (\gamma_p^R)^2$$

Equation 38

To calculate the GR using experimental data, the total released pseudo-strain energy up to failure is determined using the area under the  $W_r^R$  curve until failure (i.e., A in Eq. (36)), as depicted in Fig. 4 for a time sweep test and normalized by. The temperature independence of

the failure criterion makes it a valuable tool for predicting the performance of asphalt mixtures and binders under different loading conditions.

The PSE is employed for the computation of energy and the graphical representation of the damage curve. This study adopted the PSE S-VECD model described in Chapter 5.2 of Pseudo Strain Energy-Based Analytical Method. According to evaluations, the parameter C in the S-VECD model is derived by calculating the modulus  $|G^*(t)|$  ratio to the initial modulus  $|G^*|$ . This parameter subsequently determines the damage intensity  $D(t)$ . Determining coefficients  $C_1$  and  $C_2$  involves fitting them to the integrity-damage intensity curve, commonly called the C-D curve. Subsequently, these fitted coefficients can be substituted into the equation for parameter A. Ultimately, the fatigue life can be ascertained.

Noteworthy, distinction lies in the application of strain measurements for damage intensity calculation between the PSE S-VECD model and the S-VECD model. Specifically, the former employs pseudo strain, whereas the latter employs the total applied strain.

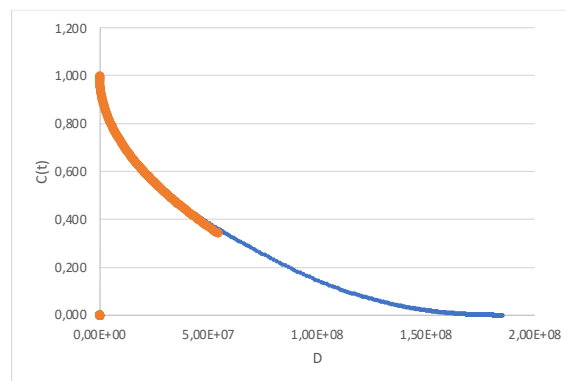


Figure 15 Example of damage model adopted on PSE S-VECD model

## **Chapter 3:**

# **EXPERIMENTAL PLAN**

### **3.1 Introduction**

This chapter presents the experimental details and tools used to evaluate the visco-elastic properties of binders. The study involved polymer-modified and unmodified asphalt binders (B and D binders are polymer-modified asphalt whereas the other binders evaluated in this study are unmodified) that were aged and tested using a dynamic shear rheometer. All binders were aged in a rolling thin-film oven and pressure aging vessel prior to testing. All tests were conducted in a DSR with an 8-mm parallel plate set-up with a 2-mm gap setting. The rheometer accurately assessed the visco-elastic properties of the binders. Linear viscoelastic characterization was conducted by systematically varying the amplitude of shear stress over a specified range at a temperature of 19 degrees Celsius, while collecting data on various rheological parameters such as complex modulus ( $G^*$ ), phase angle, and others. The study used RheoPlus software to process test results and calculate fatigue life parameters based on AASHTO standards. The fatigue life prediction model was fitted for each failure criterion and aging condition using nonlinear regression. The results were presented in a separate chapter dedicated to results and discussion. It is very important to conduct a minimum of 3 test repetitions to obtain reliable results. The use of advanced tools and techniques in this study enhances the precision and consistency of test outcomes, improves the understanding of material characteristics, and facilitates effective communication and collaboration. The findings of this study will contribute to the development of more durable and reliable bituminous binders for use in civil engineering applications.

### **3.2 Setting of the test and specimen preparation**

The dynamic shear rheometer is able to accurately assess bituminous binders and their visco-elastic properties across wide range of temperatures encountered during service. Physica MCR 302 rheometer, produced by Anton Paar Inc. has been used in this study which is illustrated in figure 16.



*Figure 16 Dynamic shear rheometer (MCR302)*

The initial stage of all testing involves the producing bitumen specimen in the mold with diameter of 8 mm seen in the figure 17.



*Figure 17 Tested binder preparation first step*

Subsequently, the mold, is placed in an oven and subjected to a temperature of 155°C for a duration of 5 minutes. Subsequently, the specimen is removed from the oven and allowed to equilibrate at ambient conditions, specifically at a temperature of around 24°C, for a duration of 5 minutes. After, Trimming is necessary to obtain the desirable sample dimension. Excessive or untrimmed material can cause errors in measurements, so both under and over-trimming are to be avoided.

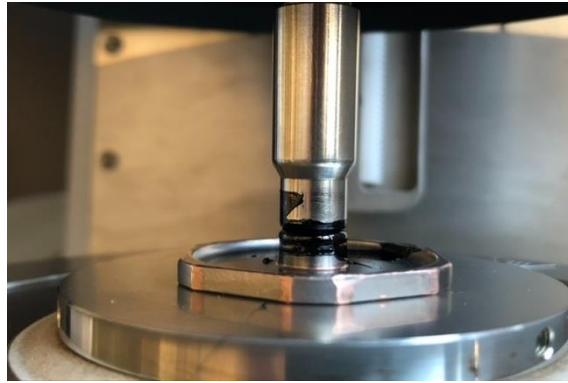


*Figure 18 Sample after the test*



*Figure 19 Adhesion problem*

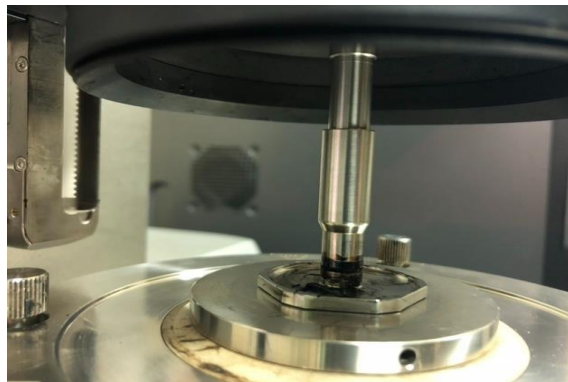


*Figure 20 Trimming of the sample*

Once the trimming process is completed, the plate is subsequently positioned for testing, during which the separation between the two plates is precisely set at a distance of 2.0 mm. Subsequently, the cover of the rheometer descends To ensure the maintenance of a stable temperature throughout the testing process. Subsequently, the examination commences. The test procedure takes approximately 30 min, including time for thermal equilibration.

### 3.3 Evaluation of the fatigue properties using data from Standard

First, test results were imported and processed using RheoPlus software, which is a special tool for studying the rheological properties of materials. The software provides several advantages, such as user-friendly interface, extensive testing functionalities, robust data analysis tools, and comprehensive reporting features. The use of RheoPlus software has the potential to enhance the precision and consistency of test outcomes, optimize the efficacy of DSR equipment testing, augment comprehension of material characteristics, and facilitate effective communication and collaboration.



Figure 21 Rheplus software interfaces.

After that, calculations based on AASHTO standards as mentioned, which include test results for asphalt binder, were carefully looked over using Microsoft Excel software. This thorough study checked if the S-VECD model could be used on DSR results of asphalt binders.

### 3.4 Calculation of Fatigue Life Parameters

This part describes the procedure for fitting the parameters of the fatigue life prediction model (Equation 25, 31, and 34) for asphalt binders under different aging and strain conditions. The steps are:

- Material properties analysis before damage applies: For the first procedure, constant amplitude oscillatory shear loading was applied at various frequencies to conduct a frequency sweep test to obtain material properties.
- Computation of the Fatigue Life for Each Failure Criterion: The fatigue life is computed for each failure criterion at each strain level using the fatigue life prediction model,

which the previous chapter discussed. To achieve this, required data for each failure criterion calculated.

- Determine the Average Values of Parameters A and B: To achieve this, a minimum of four replicates of the linear amplitude sweep (LAS) test are conducted at 19°C for each binder to determine the average values of parameters A and B. These parameters are the coefficients of the fatigue model and represent the material-specific fatigue characteristics of the binder.
- Fitting the Fatigue Model Parameters: within the last step, the fatigue model parameters are fitted for each failure criterion and aging condition using nonlinear regression. The fitted parameters are then used to predict the fatigue life of asphalt binders under different loading conditions.

## **Chapter 4:**

# **RESULTS & DISCUSSIONS**

## 4.1 Introduction

Chapter 4 of the study provides an in-depth analysis of the results obtained from a study on the fatigue characteristics of binders. This chapter aims to present the findings and discuss their implications in order to gain a comprehensive understanding of the mechanical properties and performance of the different samples. The results are obtained through laboratory testing and data calculations, and three different analysis methods are used to compare the fatigue resistance of the binders. This chapter serves as a crucial section in the article, shedding light on the influence of test conditions and aging levels on the binders' behavior.

Furthermore, the study compares the values of  $N_f$ , strain at peak,  $G^*$ , and stress at peak among the different samples and test conditions. The results reveal variations in these values, indicating the influence of test conditions and aging levels on the fatigue life and deformation behavior of the samples. This comparison provides valuable insights into how different factors can affect the mechanical properties and performance of the binders.

Additionally, the study compares the fatigue resistance of the binders at different aging levels using three distinct analysis methods. These methods include analyzing a 35% reduction in  $|G^*| \cdot \sin \delta$  as the failure criterion, evaluating maximum shear stress, and investigating pseudo strain energy. The results obtained from these methods are compared and discussed, providing a comprehensive understanding of the fatigue characteristics of the binders.

Overall, this chapter serves as a crucial component of this study, presenting the results and discussions that contribute to a deeper understanding of the mechanical properties and performance of the binders. The findings highlight the influence of test conditions and aging levels on the binders' behavior, emphasizing the importance of considering these factors in future research and practical applications.

The findings of fatigue characterization tests conducted on both unmodified and polymer-modified asphalt binders are presented in this chapter. The central emphasis lies in understanding the effects of aging and polymer modification on the fatigue characteristics of these binders. The tests involve unaged binders and have undergone aging procedures known as "RTFOT" and "PAV."

Valuable insights can be uncovered through a comprehensive analysis and making detailed comparisons. As mentioned earlier, the insights possess implications that extend beyond the confines of the laboratory, thereby providing significant contributions to the realm of civil engineering in terms of pavement design and construction practices.

The following sections of this chapter will present a comprehensive analysis of the fatigue test results and make detailed comparisons between the different binders, aging conditions, and failure criteria. The insights gained from this analysis will have important implications for designing and selecting asphalt binders.

## 4.2 Fatigue Line Parameters

According to the methods explained in Previous chapter, fatigue line parameters are calculated for all the 12 different samples with three different failure criterion analysis. These results are presented in Table 2 – Table 5 for each of the materials separately. It should be reminded; these results are the average value of the best three repetitions. These data have been used as comparison parameters in following sections to investigate the effect of aging, material type and analysis method on the fatigue resistance of fatigue binder. Moreover, based on calculated A and B parameter, the predicted number of  $N_f$  is calculated for the strain level if 2.5% as medium and more realistic strain level which can be experienced under pavement to make the comparison at intermediate strain instead of extreme values which may never experienced by the pavement. The comparison of Tables presented in 2, 3, 4, and 5 reveals variations in the values of parameters A and B,  $N_f$  among the different samples and test conditions. These variations highlight the influence of test conditions and aging levels on the mechanical properties and performance of the samples.

Sample	Aging Level	Type of Test with Failure Criterion	$N_f$ @2.5 strain level	Model Parameters	
				A	-B
A	Virgin	LAS (PSE)	4,918E+37	4,33E+05	-6,69E+00
		LAS ( $\tau_{max}$ )	4,034E+53	1,14E+06	-8,85E+00
		LAS (%35 reduction)	3,448E+130	6,15E+08	-1,49E+01
	RTFO	LAS (PSE)	7,1798E+11	1,31E+05	-2,32E+00

PAV	LAS ( $\tau_{max}$ )	1,0129E+20	6,20E+05	-3,45E+00
	LAS (%35 reduction)	1,0494E+49	9,73E+08	-5,45E+00
	LAS (PSE)	1,4939E+40	1,45E+05	-7,79E+00
	LAS ( $\tau_{max}$ )	1,2942E+94	4,91E+06	-1,41E+01
	LAS (%35 reduction)	3,985E+230	3,10E+11	-2,01E+01

Table 2 The average value of parameters A&B versus  $N_f$  (A sample).

Based on the aging characteristics of binder sample A, it was determined that most failure criteria yielded comparable results with respect to fatigue life. Specifically, it was noted that the aging of asphalt binder is associated with an increase in fatigue life at a 2.5% strain level. However, it should be mentioned that the maximum shear strain and a 35% reduction in  $G' \sin \delta$  criteria on an un-aged level resulted in a higher level of fatigue life.

About for model parameters, aging always causes an increase in number. The  $G' \sin \delta$  failure criterion, with a 35% reduction, is estimated to be the highest estimation, followed by the maximum shear strain and PSE failure criteria.

Sample	Aging Level	Type of Test with Failure Criterion	$N_f$ @2.5 strain level	Model Parameters	
				A	-B
B	Virgin	LAS (PSE)	4,57E+42	2,60E+06	-6,65E+00
		LAS ( $\tau_{max}$ )	5,69E+71	5,88E+06	-1,06E+01
		LAS (%35 reduction)	2,69E+159	4,02E+09	-1,66E+01
	RTFO	LAS (PSE)	2,7759E+44	3,97E+06	-6,73E+00
		LAS ( $\tau_{max}$ )	4,38E+85	9,84E+06	-1,22E+01
		LAS (%35 reduction)	1,294E+193	3,83E+10	-1,82E+01
	PAV	LAS (PSE)	2,6847E+43	4,41E+05	-7,69E+00
		LAS ( $\tau_{max}$ )	1,42E+126	1,60E+07	-1,75E+01
		LAS (%35 reduction)	2,3247E+43	5,44E+13	-2,35E+01

Table 3 The average value of parameters A&B versus  $N_f$  (B sample).

After conducting a thorough analysis of the binder sample B, it has been ascertained that the majority of failure criteria do not yield results that are comparable in terms of fatigue life. Specifically, it has been observed that short-term aging of asphalt binder leads to a greater increase in fatigue life at the 2.5% strain level than long-term aging. This phenomenon is

attributed to the effect of polymer modification on binder B. However, it should be emphasized that the maximum shear strain and a 35% reduction in  $G' \sin \delta$  criteria on both short and long-term aged levels resulted in a higher level of fatigue life than the PSE method.

Similarly, to sample A, the aging process invariably results in a proportional increase in the number of model parameters. Estimates indicate that the 35% reduction in  $G' \sin \delta$ , is the highest of the failure criteria, followed by the maximum shear strain and PSE criteria.

Sample	Aging Level	Type of Test with Failure Criterion	Nf @2.5 strain level	Model Parameters	
				A	-B
C	Virgin	LAS (PSE)	4,0498E+31	7,37E+04	-6,49E+00
		LAS ( $\tau_{max}$ )	7,2029E+36	7,87E+04	-7,53E+00
		LAS (%35 reduction)	4,776E+106	7,69E+07	-1,35E+01
	RTFO	LAS (PSE)	1,882E+34	1,56E+05	-6,60E+00
		LAS ( $\tau_{max}$ )	4,2189E+43	2,09E+05	-8,20E+00
		LAS (%35 reduction)	1,396E+120	2,89E+08	-1,42E+01
	PAV	LAS (PSE)	8,7056E+35	1,15E+05	-7,10E+00
		LAS ( $\tau_{max}$ )	5,0702E+59	3,95E+05	-1,07E+01
		LAS (%35 reduction)	1,053E+165	7,94E+09	-1,67E+01

Table 4 The average value of parameters A&B versus Nf (C sample).

Following a analysis of the fatigue life of binder sample C, it has been established that aging results in an increase in Nf values. The  $G' \sin \delta$  failure criterion, with a 35% reduction, has been determined to yield the highest estimation, followed by the maximum shear strain and PSE failure criteria. These findings provide insight into the performance of binder sample C and can inform further research into the properties of aging binders.

The aging process leads to an increase in the number of model parameters which also observed on previous sample binders. The highest of the failure criteria appears to be a 35% reduction in  $G' \sin \delta$ , followed by the maximum shear strain and PSE criteria. These estimates provide valuable insights into the effects of aging on the given binders.

Sample	Aging Level	Type of Test with Failure Criterion	N <sub>f</sub> @2.5 strain level	Model Parameters	
				A	-B
<b>D</b>	Virgin	LAS (PSE)	3,04E+37	5,21E+05	-6,56E+00
		LAS ( $\tau_{max}$ )	1,78E+50	7,75E+05	-8,53E+00
		LAS (%35 reduction)	2,71E+130	9,44E+08	-1,45E+01
	RTFO	LAS (PSE)	1,4217E+39	7,86E+05	-6,64E+00
		LAS ( $\tau_{max}$ )	2,0125E+55	9,21E+05	-9,27E+00
		LAS (%35 reduction)	1,924E+145	2,95E+09	-1,53E+01
	PAV	LAS (PSE)	1,7906E+12	1,19E+05	-2,41E+00
		LAS ( $\tau_{max}$ )	5,1404E+25	1,03E+06	-4,28E+00
		LAS (%35 reduction)	2,387E+67	5,44E+10	-6,28E+00

Table 5 The average value of parameters A&B versus N<sub>f</sub> (D sample).

It is interesting to note that the analysis of binder sample D has revealed that most of the failure criteria do not produce comparable results in terms of fatigue life within aging conditions. Specifically, it has been observed that short-term aging of asphalt binder leads to a greater increase in fatigue life at the 2.5% strain level, followed by unaged aging level of asphalt binder B. It is not expected that fatigue life will decrease with long term aging. This phenomenon is attributed to the effect of modification on binder D. Similarly, with other binder samples, it should be emphasized that the maximum shear strain and a 35% reduction in  $G' \sin \delta$  criteria resulted in a higher level of fatigue life than the PSE method.

Model parameters A and B resulted in an increase in aging. Similarly, observation continues on binder D, in which the highest of the failure criteria appears to be a 35% reduction in  $G' \sin \delta$ , followed by the maximum shear strain and PSE criteria on model parameters.

In conducting a comprehensive analysis of a range of asphalt binder samples (designated A, B, C and D), which were subjected to distinct aging conditions and fatigue life criteria, several key observations have emerged. Notably, the aging process has resulted in a consistent increase in N<sub>f</sub> values across A and Samples, indicating superior fatigue life than that of sample binder C and D. Model parameters A and B exhibit significant variations among the different samples and aging conditions, underscoring the impact on failure criterion evaluation of the binders.

Specifically, short-term aging tends to lead to a notable boost in fatigue life, as observed in samples B and D at the 2.5% strain level. On the other hand, it is surprising to observe a decrease in fatigue life with long-term aging on sample D, which is likely influenced by polymer modifications. These findings suggest that the impact of aging conditions on asphalt binder samples and their resulting fatigue life merits further investigation, particularly in the context of long-term aging with modified asphalt binders, which can have unexpected and potentially deleterious effects on binder performance.

Furthermore, the analysis highlights that the 35% reduction in  $G^* \sin \delta$  criterion consistently yields higher estimations for fatigue life and model parameters across all samples, followed by the maximum shear strain criterion, while the PSE method typically provides lower estimations. This trend indicates the significance of the selected failure criteria in assessing the fatigue life of asphalt binders.

### **4.3 Comparison of Fatigue resistance at different aging level**

In order to achieve the overarching goal, three distinct analysis methods are utilized, each providing unique perspectives on the behavior of the binders. The study implements methodologies to evaluate a 35% reduction in  $|G^*| \cdot \sin \delta$ , analyze maximum shear strain, and investigate pseudo strain energy. This study employs a multifaceted approach to comprehensively investigate the influence of aging on the fatigue characteristics of binders. Moreover, this study aims to clarify any discrepancies or associations among the outcomes produced by the various analysis methods employed.

#### **4.3.1 Analysis based on %35 Reduction in $|G^*| \cdot \sin \delta$ Failure Criteria**

Fatigue line diagrams related to each of the investigated binders (A, B, C, and D) are used in this section to facilitate the comparison of the results. Figure 22 is presenting the results related to the analysis based on fatigue failure of 35% reduction in  $|G^*| \cdot \sin \delta$ .

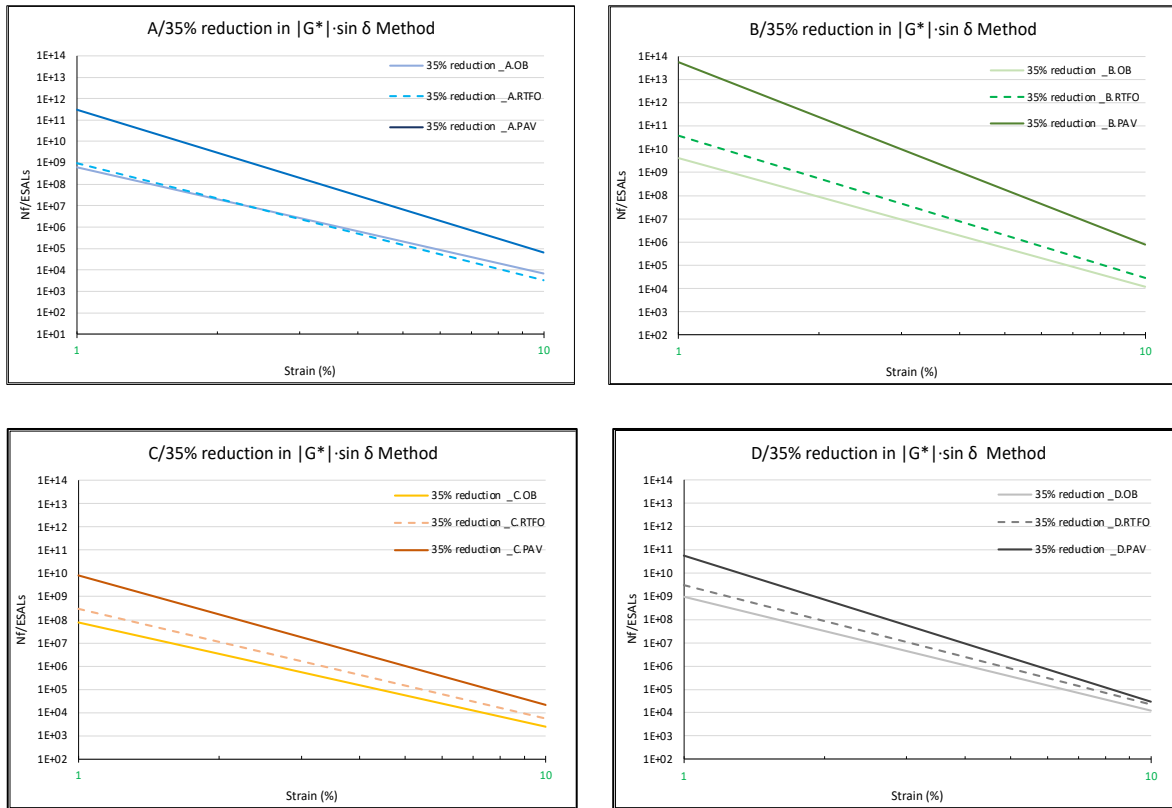


Figure 22 Resulted from %35 reduction in  $|G^*| \cdot \sin \delta$  failure criteria.

According to results presented in previous figures, it can be stated in most cases, the long-term aged binders show the highest fatigue resistance while the lowest fatigue life are observed in the non-aged materials. Except sample D in the RTFO aging level, it is observed the use of 35% reduction in  $|G^*| \cdot \sin \delta$  as the failure criterion is resulting in highlighted effect of the aging. In particular, using this method is showing the more aged binders have a better resistance to aging distress which is not the expected conclusion. This phenomenon can be explained by the fact that the more aged binder has higher stiffness which resulted in higher value in calculation of A parameter. In other words, A parameter is calculated based on  $C_0$  and  $C_1$ , where both are directly related to the stiffness of the binder. In this regard, use of this failure criterion seems not proper to compare the effect of aging in analysing LAS results.

### 4.3.2 Analysis based on Maximum Shear Stress Failure Criteria

Following part, a comprehensive analysis of the results obtained from the maximum shear stress failure criterion on individual samples of asphalt binders A, B, C, and D are presented.

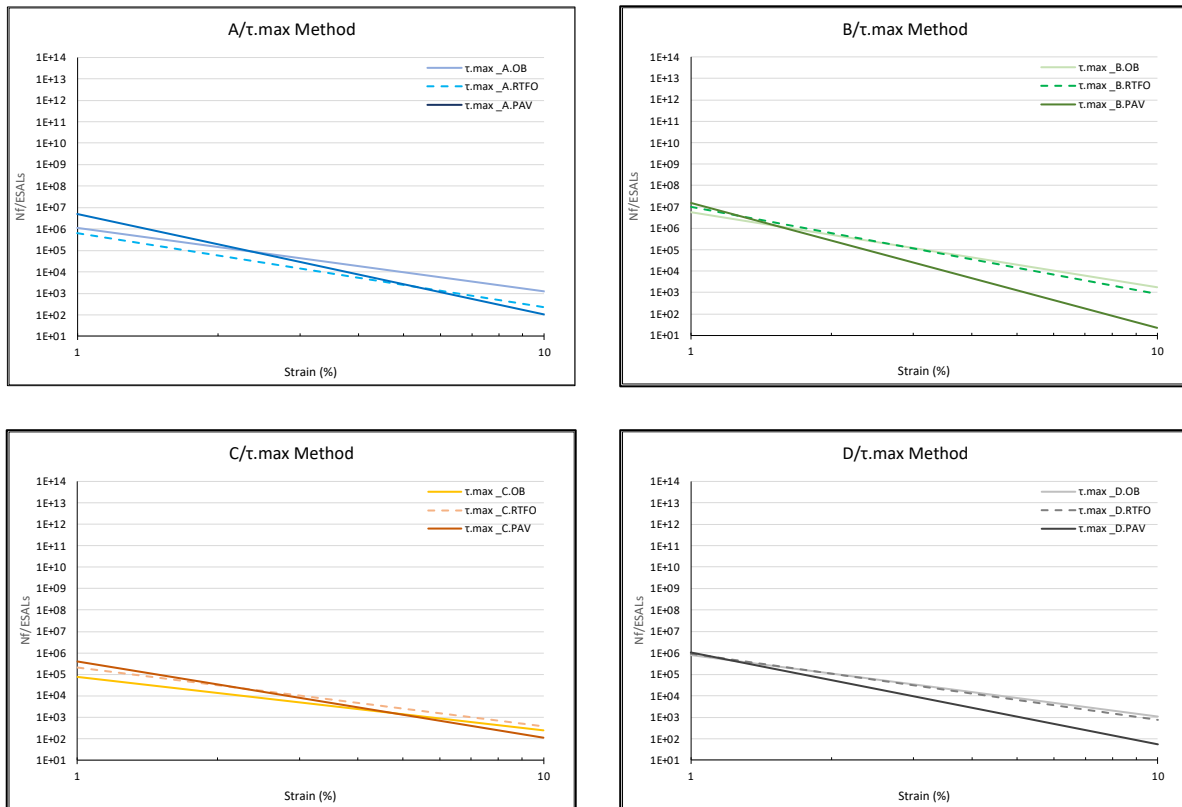


Figure 23 Resulted from max shear strain failure criteria.

The maximum shear strain failure criterion shows a different trend compared to the 35% reduction in  $|G^*| \cdot \sin \delta$  failure criterion. In particular, long-term aged binders are not always the most resistant to fatigue. Results show that in most cases, the PAV-aged sample only exhibits the highest resistance at lower strain levels. At higher strain levels, the non-aged binder is always more resistant to fatigue. Material C is less sensitive to aging when analyzed by this method, following a virtually indistinguishable at different aging levels. In general, this method shows that at high strain levels, non-aged binders have better fatigue resistance, which is the anticipated outcome.

This suggests that the maximum shear strain failure criterion may be more appropriate for comparing the effect of aging on the fatigue life of asphalt binders, particularly at high strain levels. This is because the maximum shear strain failure criterion is based on the idea that fatigue damage is caused by the accumulation of shear stress in the asphalt binder. At high strain levels, the shear stress in the asphalt binder is high, regardless of the aging condition.

Therefore, the non-aged binder, which is more ductile, is more resistant to fatigue at high strain levels.

### 4.3.3 Analysis based on Pseudo Strain Energy Failure Criteria

A comprehensive analysis of the results obtained from the PSE criterion on individual asphalt binder samples A, B, C, and D will be conducted. The PSE criterion is a widely used method for evaluating the performance of asphalt binders under different conditions. The objective of this analysis is to provide a better understanding of the properties of each binder and to identify their potential applications.

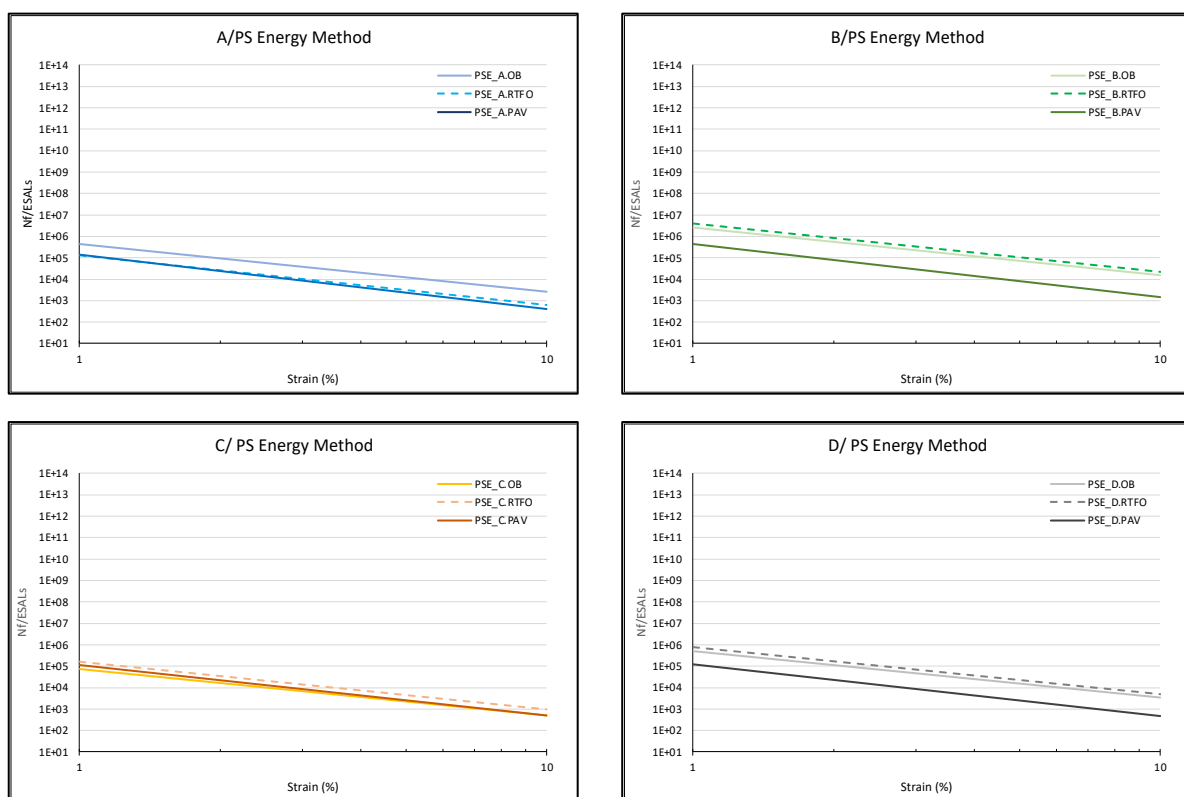


Figure 24 Resulted from pseudo strain energy failure criteria.

According to the maximum pseudo strain energy failure criterion, unaged and short-term aged binders follow almost the same trends and consistently have better fatigue life than long-aged binders. The material C is less susceptible to aging when analyzed by this method, which is consistent with previous observations. It is worth noting that virgin level binders exhibit better resistance to aging distress, as expected.

The overall analysis of this part will be considered as, starting with observing the difference in fatigue life among various aging conditions. Experimental results on the maximum shear stress method show opposite results between high and low strain levels. The maximum shear stress methods at high strain levels and pseudo strain energy failure criterion show higher fatigue life on non-aged binders. In contrast, the second failure criteria at low strain levels and the first failure criteria underestimate the fatigue life of binders, which shows higher fatigue life on long-term aged binders. This indicates that there is a difference in total damage input when calculating the fatigue life of asphalt binders using these three methods. The findings of this study suggest that the pseudo strain energy failure criterion is the most appropriate method for calculating the fatigue life of asphalt binders.

Other studies provide further support for these findings, indicating that the pseudo-strain energy-based analytical approach is theoretically more accurate in representing damage growth compared to other methods. This pseudo-strain energy-based method separates the viscoelastic properties of asphalt materials from the damage test, allowing for a standalone analysis of damage development [9].

Briefly, the aging phenomenon of asphalt pavement during construction and use impacts the fatigue resistance of asphalt binders. Therefore, it is essential to research the fatigue resistance of aged asphalt binders when designing, building, and maintaining asphalt pavements. This research highlights the intricate dynamics at play and reinforces the importance of selecting an appropriate analysis method in accurately assessing the effect of aging on asphalt binders.

#### **4.4 Comparison of Different Failure Criteria**

This section presents a detailed comparison of fatigue resistance results of asphalt binders A, B, C, and D that were subjected to different analysis methods. To understand the subtle effects of these failure criteria on the binders' fatigue life predictions, the binders are examined under uniform aging conditions. The purpose of this section is to clarify the differing behaviors that these failure criteria present when describing the fatigue resistance of different samples. To this aim, Figure 25 to Figure 28 are presenting fatigue lines obtained from the LAS result analyses based on the considered failure criteria: maximum shear stress according to AASHTO TP101-14, pseudo strain energy failure, and 35% reduction in  $|G^*| \cdot \sin \delta$  in accordance to the latest update of AASHTO standard (T391-20).

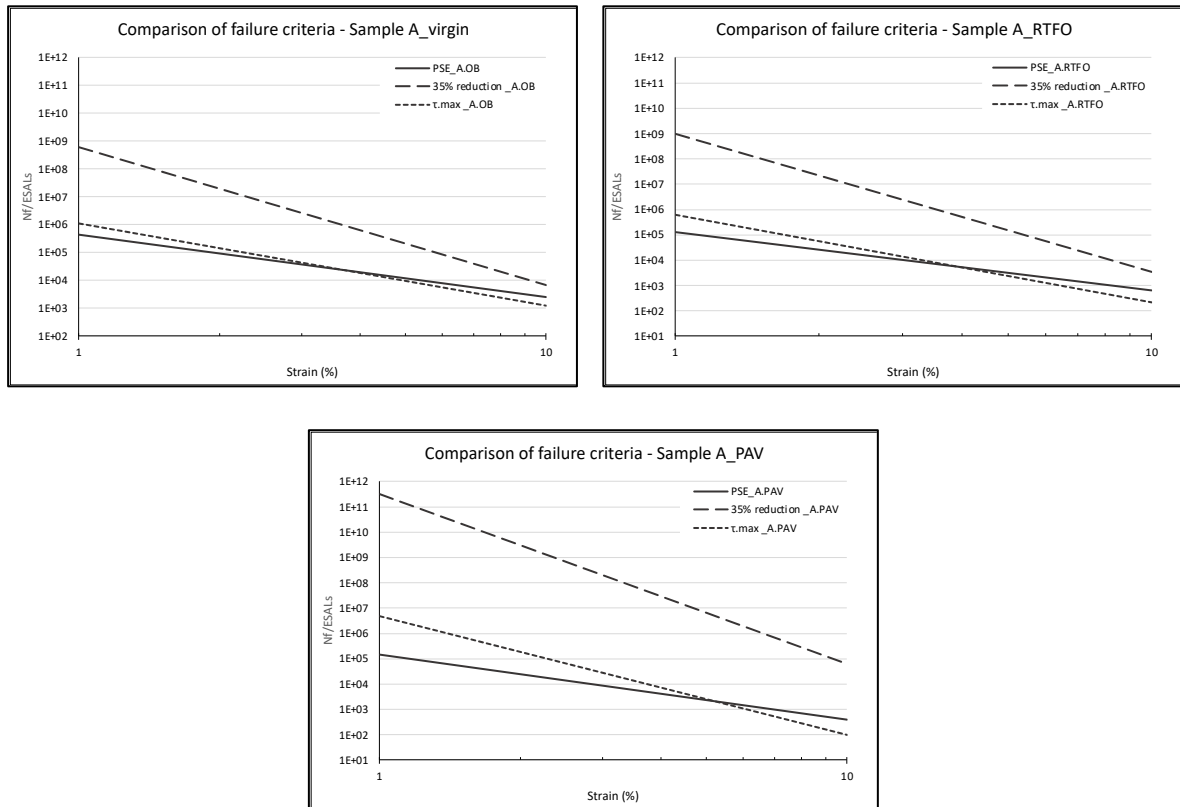


Figure 25 Resulted from using different failure criteria (Sample A)

Figure 25 is presenting the fatigue life estimation of asphalt binder sample A which evaluated by use of three different failure criteria. Results indicate that the max pseudo strain energy criterion and maximum shear stress failure criterion produced comparable estimates in comparison to the 35% reduction in  $|G^*| \cdot \sin \delta$  which produced notably higher estimation. The outcomes suggest that a comprehensive evaluation of an asphalt binder's fatigue performance should consider multiple criteria. The 35% reduction in  $|G^*| \cdot \sin \delta$  criterion appears to be more conservative, highlighting the nuanced nature of assessing fatigue behavior. Through this study, it is evident that the interpretation of fatigue behavior of asphalt binder is complex and requires careful consideration of multiple criteria.

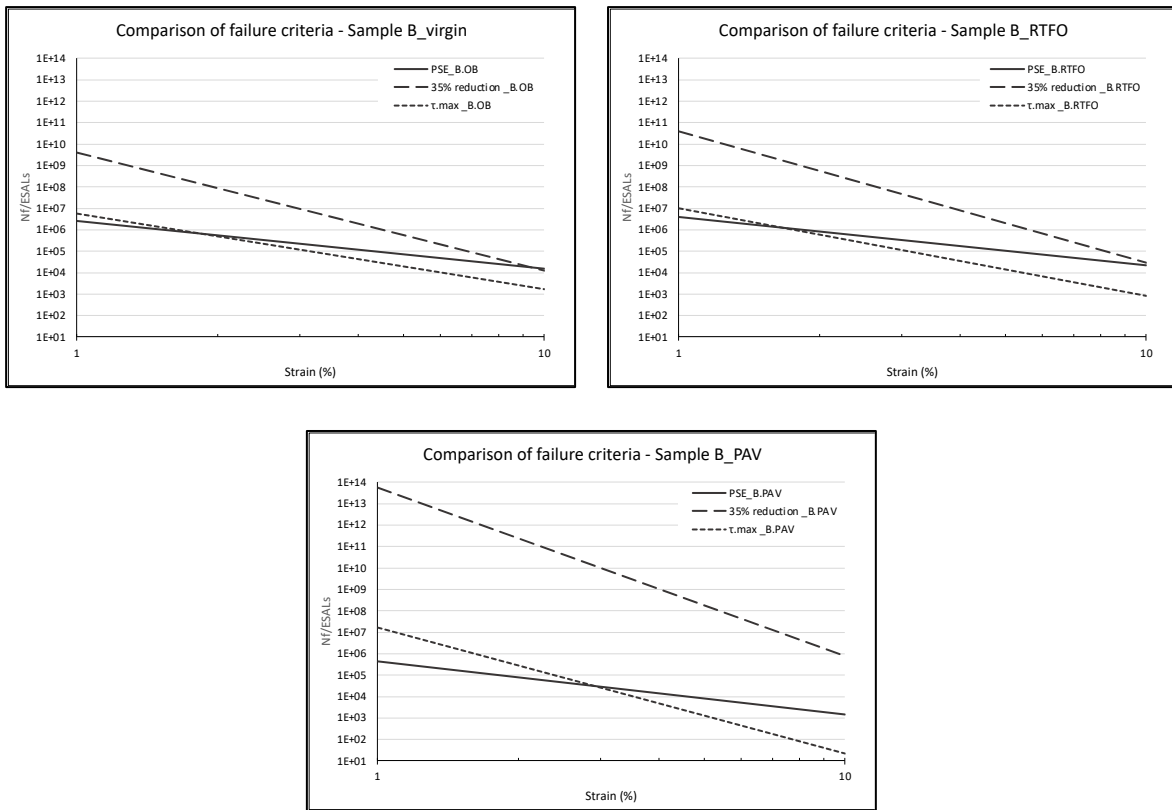


Figure 26 Resulted from using different failure criteria (Sample B).

Asphalt binder B shows similar trends in all three failure criteria for unaged and short-term aged binders. The 35% reduction in  $|G^*| \cdot \sin \delta$  consistently estimates a higher fatigue life compared to other methods. When we analyze the strain levels, some important observations come to light. At a critical strain level of 4.5%, we notice that the maximum shear strain method gives higher estimates of fatigue life when the strain is below this threshold. On the other hand, the pseudo strain energy method predicts higher fatigue life when the strain exceeds 4.5%.

In the context of long-term aged binder B, a 35% reduction in the  $|G^*| \cdot \sin \delta$  failure criterion has resulted in notable variations in performance predictions. Specifically, this criterion has been demonstrated to generate significantly higher estimates, leading to longer fatigue life projections. In contrast, the maximum shear strain failure criterion tends to predict a shorter fatigue life, particularly at high strain levels. Hence, it is imperative to exercise discretion in the selection and application of the appropriate criterion when forecasting the fatigue life of long-term aged binder B.

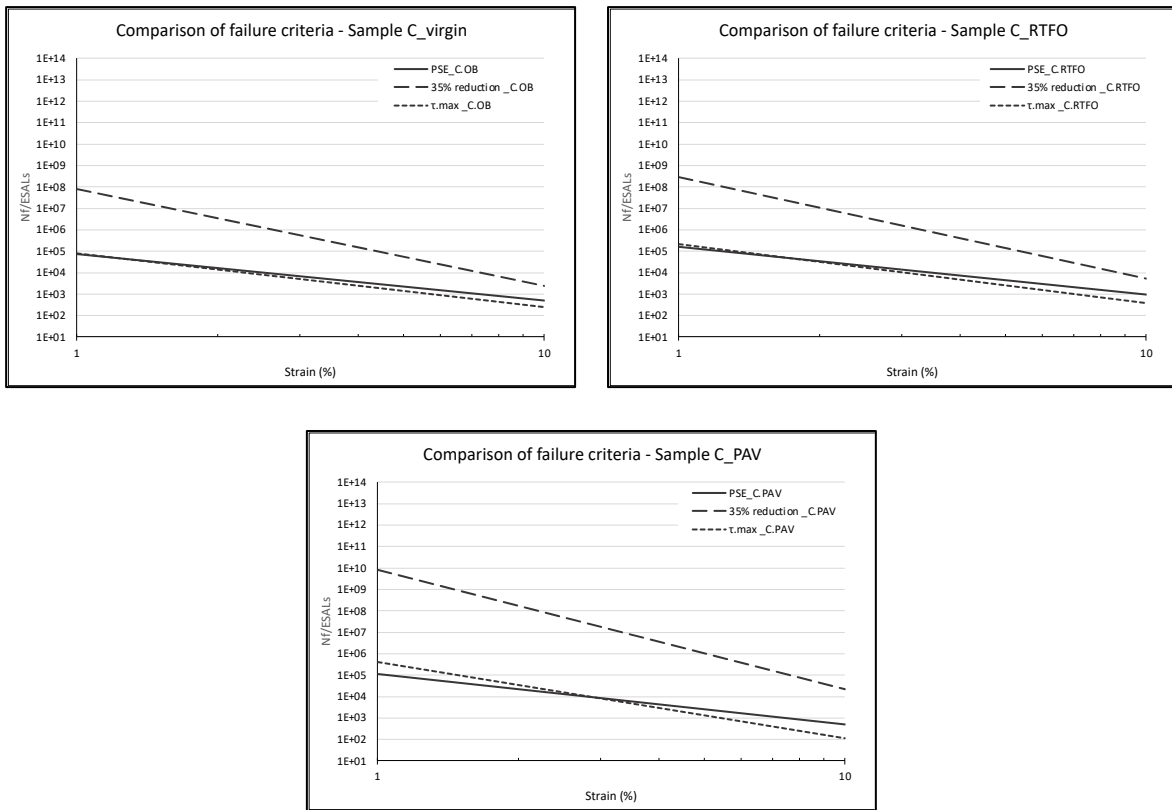


Figure 27 Resulted from using different failure criteria (Sample C).

Binder C has been studied under different failure criterion conditions, and it has been noticed that the same trends continue to persist. The estimation of value on the 35% reduction in  $|G^*| \cdot \sin \delta$  failure criterion is of greater significance, followed by slightly similar values on the maximum shear strain and pseudo strain failure criteria.

In comparison to the other samples, it is noteworthy that the estimated trends for the failure criteria exhibit consistency across unaged, short-term aged, and long-term aged conditions. This continuity suggests that the performance characteristics of binder C demonstrate a robustness that persists despite variations in aging, underscoring its stability and reliability under diverse conditions.

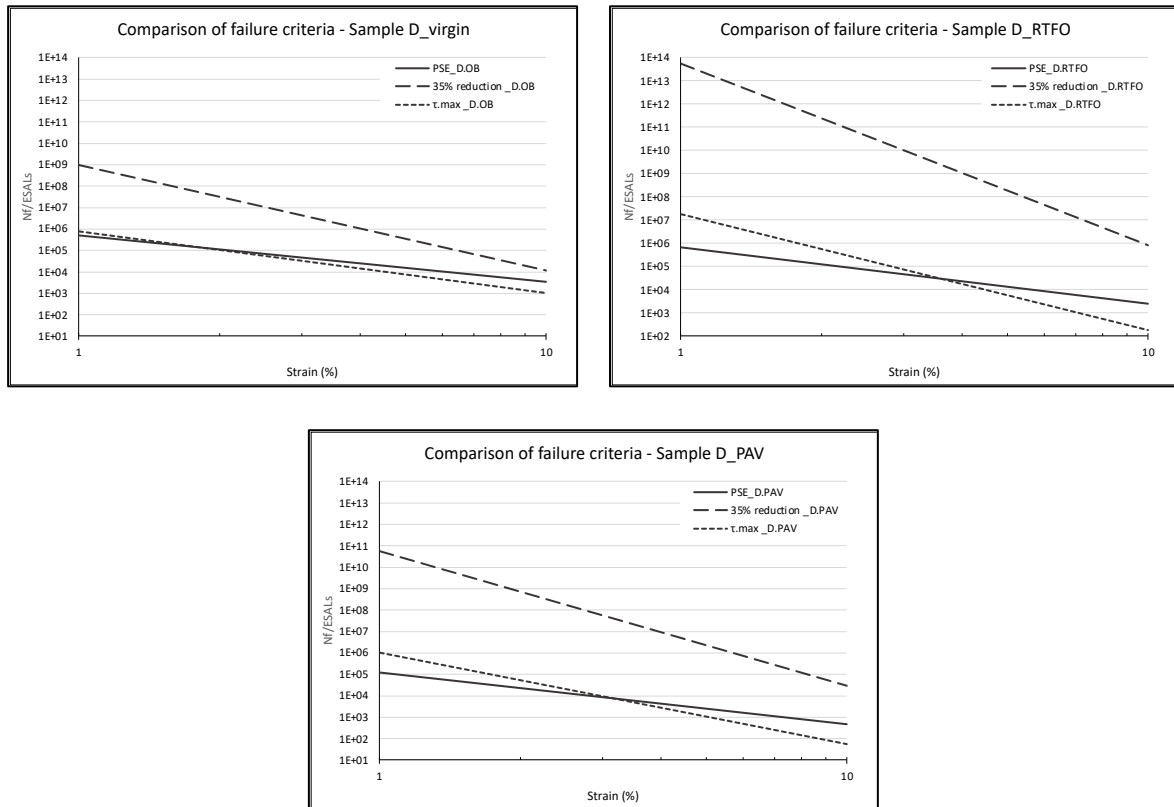


Figure 28 Resulted from using different failure criteria (Sample D)

Asphalt binder D displays a consistent trend across all three failure criteria for unaged and long-term aged binders. Notably, the 35% reduction in  $|G^*| \cdot \sin \delta$  method consistently estimates a higher fatigue life compared to other methods. Analysis of strain levels revealed important observations. Notably, the maximum shear strain method gives higher estimates of fatigue life when the strain is below a critical threshold of 5%. Conversely, the pseudo strain energy method predicts higher fatigue life when the strain exceeds 5%. These findings suggest that Asphalt binder D is a robust material with predictable fatigue life. It is advised to employ the 35% reduction in  $|G^*| \cdot \sin \delta$  technique while estimating the fatigue life of Asphalt binder D, particularly on Pav aged, in future studies that lack precision. This method has proven to be effective in obtaining accurate results.

When contemplating the short-term behavior of aged binder D, a noteworthy variation in performance predictions has been observed as a result of a 35% reduction in the  $|G^*| \cdot \sin \delta$  failure criterion. Specifically, this criterion has exhibited a tendency to generate significantly higher estimates, which have led to longer fatigue life projections.

The findings of all chosen binders A, B, C, and D provide compelling evidence that the fatigue life estimated using a 35% reduction in  $|G^*| \cdot \sin \delta$  failure criterion is substantially higher than any other failure criteria. The failure criterion in question, particularly with respect to the modified asphalt (B, D) binder over an aging period, yields significantly higher values than other criteria. This observation underscores the criticality of assessing the longevity of binders used in asphalt modification and the need to establish more robust performance standards.

In the context of non-aged asphalt binders, for all the four samples, the maximum shear stress and PSE method present a similar trend across all failure criteria. This observation highlights the functional equivalence of these two methods in this setting. It is worth noting that the failure criteria under consideration are not distinguished under the aforementioned methods.

In contrast to this study's findings on failure criteria, recent literature suggests that the pseudo-strain energy-based method produces a slightly higher fatigue life as compared to other failure. The research underlines the reason by referring criteria methods across the entire loading strain range described in Equation 25. The observed discrepancy in damage input between the three failure criterion in calculating the total damage intensity of asphalt binders is diverse [9].

This finding has significant implications in the asphalt binder industry as it highlights the need to carefully consider the choice of the fatigue life determination method. Given the difference in fatigue life predictions between the three methods, it is crucial for researchers and industry professionals to be aware of the potential impact of their choice of method on the performance of asphalt binders. To fully understand the differences in predictions between failure criteria, further research is essential.

#### **4.5 Comparison of binder type**

According to the availability of results for different binder types in this study and the interest in comparing the effect of fatigue failure criteria on the final fatigue resistance of these binders, there is a possibility to compare the four tested samples in term of their fatigue life. This study aims to compare the fatigue characteristics exhibited by asphalt binders sourced from diverse refineries and impacted by different geological conditions while also considering the impact of different aging conditions. In order to compare, three failure criteria were used on four different

asphalt binders at the same aging levels. The achievement is on these studies to acquire significant knowledge regarding the impact of polymer modification effect on binders.

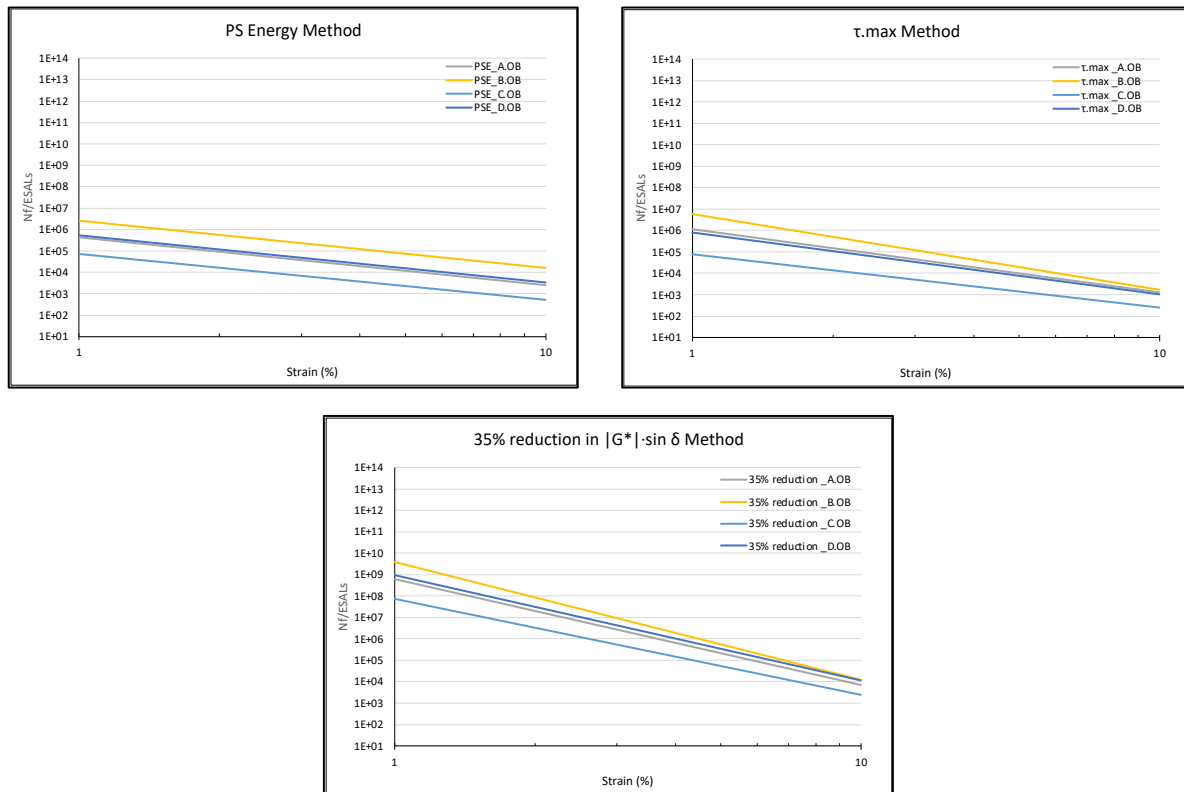


Figure 29 Resulted from unaged samples using all failure criteria.

According to the results presented in Figure 29 for unaged binders, it has been observed that modified binders B and D exhibit a greater resistance to fatigue than unmodified asphalt binder A and C. On the other hand, asphalt binder C has been found to have the least fatigue life. A noteworthy trend is observed with respect to the maximum shear strain method estimation, particularly in the case of binder A, where the estimation is only slightly higher than that of binder D. In addition, asphalt binder B has been found to exhibit the best fatigue life among all the binders studied. This discovery has significant implications for the design and construction of asphalt pavements since using modified binder B can improve the pavement's durability and lifespan. It is important to note, however, that further studies are needed to explore the full potential of modified binders in improving the performance of asphalt pavements.

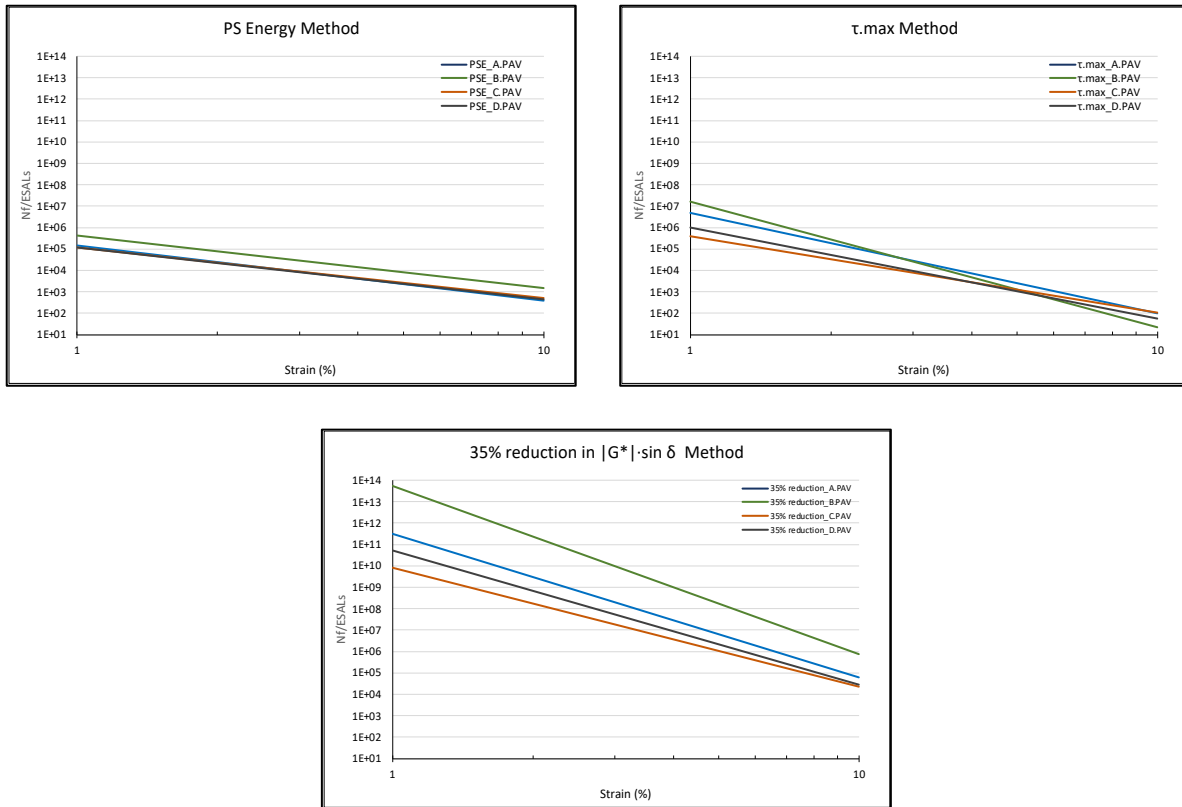


Figure 30 Resulted from long-term aged samples using all failure criteria.

In the context of long-term aged samples, it is commonly observed that polymer-modified asphalt binder B exhibits better fatigue life compared to others, similar to unaged binders. However, the maximum shear strain method at a high strain level reveals that sample binder B has a lower fatigue life than other samples. This phenomenon may be attributed to the fact that the maximum shear strain method tends to overestimate at high strain levels, particularly with an increase in aging.

Furthermore, results from the graphs illustrate a 35% reduction in  $|G^*| \cdot \sin \delta$  failure criterion estimates within aging, indicating a higher value and an unexpected outcome. This evidence suggests that the 35% reduction in  $|G^*| \cdot \sin \delta$  is not a reliable indicator to characterize the fatigue performance of asphalt binders, especially for modified asphalt binders.

Moreover, it is noteworthy that modified asphalt binder D exhibits resembling fatigue performance to neat binder A and C. The similarity in mechanical response between modified and unmodified binders can be attributed to the effect of aging. It is a well-established fact that aging can cause the mechanical response of binders to become similar.

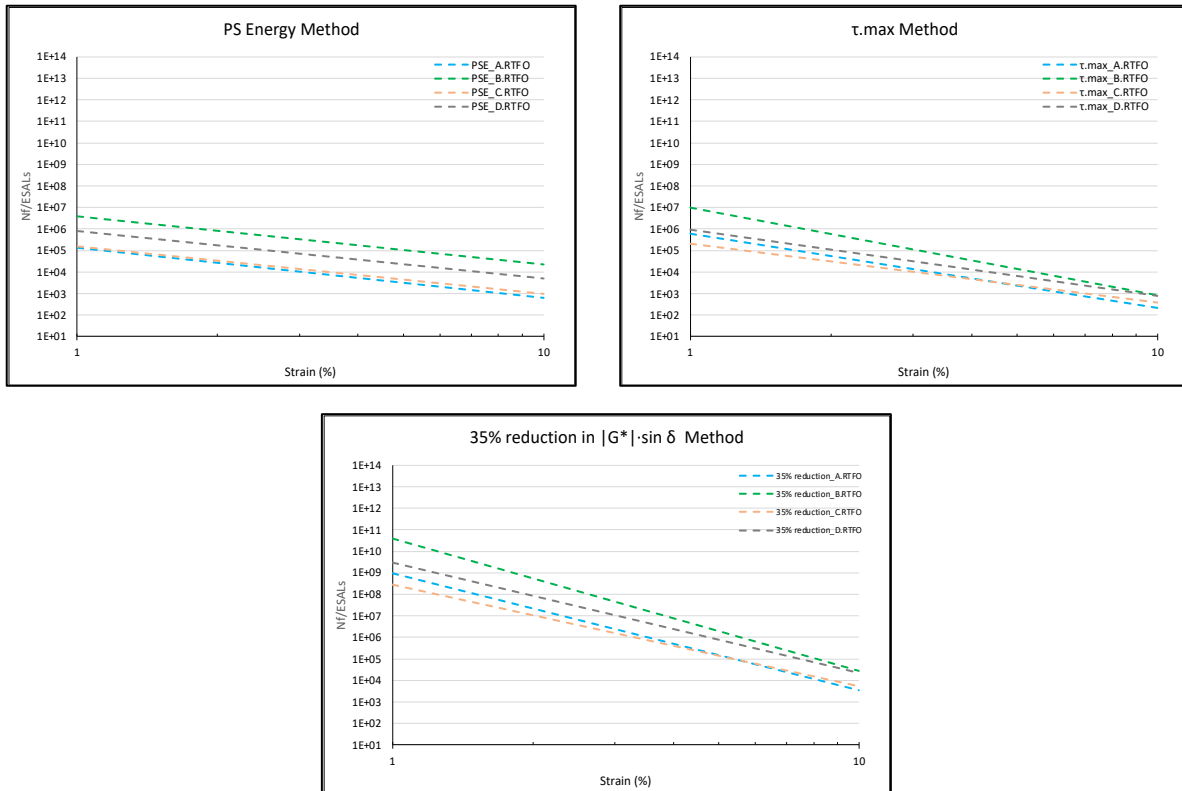


Figure 31 Resulted from short-term aged samples using all failure criteria.

Under the conditions of short-term aging, similarly to previous findings, the PMB (Polymer Modified Binders) of type B and D have a better fatigue life compared to the neat binders A and C. Unlike the unaged binders, sample D has a better fatigue life than sample A, which is distinguishable. Similarly, with long-term aged asphalt binders, there is a 35% reduction in the  $|G^*| \cdot \sin \delta$  failure criterion, leading to higher estimates within aging.

Overall, the results suggest that polymer-modified binder B has the best fatigue life of all the binders studied, regardless of aging condition. Modified binder D also exhibits good fatigue resistance, but it is less sensitive to aging than modified binder B. Unmodified binders A and C have the worst fatigue resistance, and they are more susceptible to aging. Briefly, the modified binders exhibited significantly greater fatigue resistance than the neat binders which is expected results is obtained.

The maximum shear strain approach may not provide a reliable means of evaluating the fatigue durability of asphalt binders, particularly those that are modified and subjected to higher strain levels. Additionally, the 35% decrease in the  $|G^*| \cdot \sin \delta$  failure criterion cannot be considered a dependable indicator of the fatigue performance of modified binders.

## 4.6 Comparison on different scenarios

In this section, some comments on different scenarios are made based on the results of the analyses made in this study and the conclusions in similar literatures. This study includes different methods to interpret data from asphalt binder fatigue tests are compared, depending on the specific scenarios of the binder.

Stored pseudo strain energy depends on modification of binder:

The challenge of identifying the peak values of stored pseudo-strain energy in modified asphalt binders has been widely acknowledged by researchers. This challenge poses a significant obstacle in utilizing the pseudo-strain energy failure criterion for the accurate prediction of the fatigue life of such binders. According to this criterion, fatigue failure occurs when the stored pseudo-strain energy reaches its peak. However, the difficulty in identifying the peak value of stored pseudo-strain energy hinders the determination of when exactly fatigue failure will occur. These concerns warrant attention and further investigation to improve the understanding and prediction of the fatigue life of modified asphalt binders.

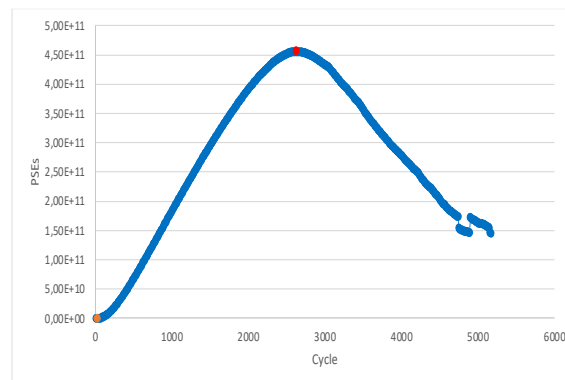


Figure 32 Resulted from unaged binder B using PSE failure criteria.

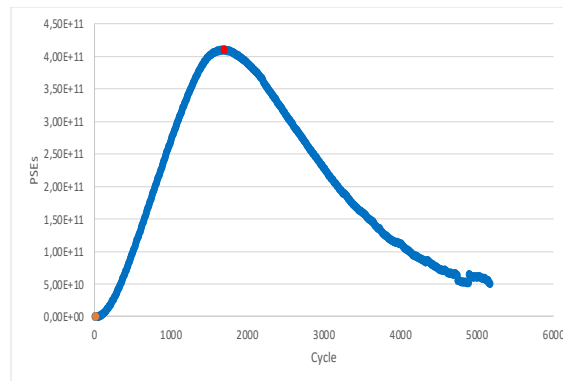


Figure 33 Resulted from unaged binder D using PSE failure criteria..

Based on the test results, it can be observed that both types of modified binders display a maximum point in the stored pseudo strain energy when they are in an unaged condition. This observation not only addresses the challenge noted by several authors in the literature but also sheds light on a potential key parameter for binder characterization. The consistency of this phenomenon in types of modified binders underlines its reliability and practicality on PS energy failure criterion.

- Aging depends on damage parameter and complex modulus:

The accurate prediction of the tolerance of asphalt binders' fatigue life and aging time holds considerable significance in the realm of asphalt binder performance evaluation. In the present study, we aim to investigate the influence of aging levels of selected asphalt binders on  $G^*$ , model parameters (A and B) on same failure criterion evaluations. Furthermore, we will delve into the examination of tolerance on strain level concerning the model parameters A and B.

The complex modulus of asphalt binder typically increases as it ages, which follows established failure criteria. For instance, referring to Table 6 of the PSE method, it can be observed that Sample B exhibits a complex modulus of  $4.10E+07$  under short-term aging whereas this value increases to  $8.14E+07$  under long-term aging. Upon examining the data presented in this table, it is evident that the PSE failure criterion shows a higher value of the model parameter A at the virgin level. This finding suggests that at an unaged level, the material under consideration exhibits a greater resistance to fatigue at lower strain levels. On the other hand, model parameter B is high for RTFO level aged binders. This indicates that these binders are highly sensitive to strain level at these ages.

Upon analysis, it is evident that there is a clear association between parameter A and aging, as it tends to follow a similar trend as  $G^*$ , with higher values as aging increases, suggesting a positive correlation. On table 7 at maximum shear strain method, it can be observed that sample B at long-term aged condition has  $1,60E+07$ , higher value of parameter A than the other samples due to its higher  $G^*$  value, is  $8,14E+07$ . Binder B exhibits a higher value of model parameter A, which results in higher fatigue resistance at lower strain levels, particularly on PAV-level aging. In contrast, model parameter B on the maximum shear failure criterion does not have a consistent relationship with aging and is not sensitive to strain level.

Unlike parameter A, parameter B exhibits a distinct and negative relationship with aging, resulting in lower values as aging progresses. This relationship is illustrated in Table 8, which shows the effects of long-term aging on the 35% reduction in  $|G^*| \cdot \sin \delta$  method in sample D. Specifically, un-aged sample D has a  $G^*$  value of  $3.48E+07$  and an average B parameter of  $-1.45E+07$ . However, after long-term aging, the  $G^*$  value increases to  $3.99E+07$ , and the average B parameter becomes  $-1.53E+07$ . After conducting a thorough analysis, we found that the 35% reduction in the  $|G^*| \cdot \sin \delta$  failure criterion leads to a higher value of the model parameter A at the PAV-aged level. This aging process results in higher fatigue resistance at a lower strain level. However, in the case of the likely maximum shear strain failure criterion, the model parameter does not have a consistent relationship with aging.

Type of Test with Failure Criterion	Aging Level	Sample	$G^*$ @10Hz	Strain @peak	Stress @peak	Model	Parameters
			[Pa]	[%]	[Pa]	A	-B
LAS-PSE	Virgin	A	$1,60E+07$	$4,15E+01$	$9,28E+05$	$1,52E+02$	$-6,69E+00$
		B	$3,00E+07$	$7,42E+01$	$1,20E+06$	$1,31E+02$	$-6,65E+00$
		C	$3,29E+07$	$2,38E+01$	$1,27E+06$	$1,56E+02$	$-6,49E+00$
		D	$3,48E+07$	$4,47E+01$	$1,57E+06$	$1,50E+02$	$-6,56E+00$
	RTFO	A	$7,44E+06$	$1,27E+01$	$3,53E+05$	$4,47E+01$	$-2,32E+00$
		B	$4,10E+07$	$8,33E+01$	$1,29E+06$	$1,14E+02$	$-6,73E+00$
		C	$3,74E+07$	$3,04E+01$	$1,57E+06$	$1,47E+02$	$-6,60E+00$
		D	$3,99E+07$	$5,06E+01$	$1,50E+06$	$1,38E+02$	$-6,64E+00$
	PAV	A	$5,15E+07$	$2,71E+01$	$1,88E+06$	$1,03E+02$	$-7,79E+00$
		B	$8,14E+07$	$3,08E+01$	$2,19E+06$	$8,45E+01$	$-7,69E+00$

C	6,51E+07	2,54E+01	2,23E+06	1,20E+02	-7,10E+00
D	7,33E+07	3,41E+01	2,37E+06	1,08E+02	-2,41E+00

Table 6 Summary parameter obtained from LAS-PSE failure criterion.

Type of Test with Failure Criterion	Aging Level	Sample	G* @10Hz	Strain @peak	Stress @peak	Model	Parameters
			[Pa]	[%]	[Pa]	A	-B
LAS- $\tau_{max}$	Virgin	A	1,60E+07	3,62E+01	9,79E+05	1,14E+06	-8,85E+00
		B	3,00E+07	4,68E+01	1,37E+06	5,88E+06	-1,06E+01
		C	3,29E+07	2,06E+01	1,35E+06	7,87E+04	-7,53E+00
		D	3,48E+07	3,52E+01	1,70E+06	7,75E+05	-8,53E+00
	RTFO	A	7,44E+06	1,06E+01	3,78E+05	6,20E+05	-3,45E+00
		B	4,10E+07	3,80E+01	1,56E+06	9,84E+06	-1,22E+01
		C	3,74E+07	2,56E+01	1,68E+06	2,09E+05	-8,20E+00
		D	3,99E+07	3,30E+01	1,78E+06	9,21E+05	-9,27E+00
	PAV	A	5,15E+07	2,29E+01	2,00E+06	4,91E+06	-1,41E+01
		B	8,14E+07	2,05E+01	2,39E+06	1,60E+07	-1,75E+01
		C	6,51E+07	2,10E+01	2,38E+06	3,95E+05	-1,07E+01
		D	7,33E+07	2,58E+01	2,58E+06	1,03E+06	-4,28E+00

Table 7 Summary parameter obtained from LAS-  $\tau_{max}$  failure criterion.

Type of Test with Failure Criterion	Aging Level	Sample	G* @10Hz	Strain @peak	Stress @peak	Model	Parameters
			[Pa]	[%]	[Pa]	A	-B
LAS- %35 reduction in $ G^*  \cdot \sin \delta$	Virgin	A	1,60E+07	3,01E+01	9,41E+05	6,15E+08	-1,49E+01
		B	3,00E+07	2,29E+01	1,22E+06	4,02E+09	-1,66E+01
		C	3,29E+07	2,07E+01	1,34E+06	7,69E+07	-1,35E+01
		D	3,48E+07	2,53E+01	1,62E+06	9,44E+08	-1,45E+01
	RTFO	A	7,44E+06	8,93E+00	3,67E+05	9,73E+08	-5,45E+00
		B	4,10E+07	2,15E+01	1,46E+06	3,83E+10	-1,82E+01
		C	3,74E+07	2,36E+01	1,67E+06	2,89E+08	-1,42E+01
		D	4,19E+07	2,52E+01	1,84E+06	2,95E+09	-1,53E+01
	PAV	A	5,15E+07	2,32E+01	1,99E+06	3,10E+11	-2,01E+01
		B	8,14E+07	2,12E+01	2,38E+06	5,44E+13	-2,35E+01
		C	6,51E+07	2,15E+01	2,38E+06	7,94E+09	-1,67E+01
		D	7,33E+07	2,28E+01	2,56E+06	5,44E+10	-6,28E+00

Table 8 Summary parameter obtained from LAS- %35 reduction in  $|G^*| \cdot \sin \delta$  failure criterion.

This study provides valuable insights into the impact of aging on asphalt binders' fatigue life and model parameters. The findings can aid in designing and constructing asphalt pavements more accurately and developing precise fatigue prediction models.

- Peak phase angle depends on modification of binder:

In comparison to the other two modified binders, the peak phase angle of the neat binder demonstrates the highest value.

## **Chapter 5:**

# **CONCLUSION**

In conclusion, this thesis focused on the fatigue characterization of bituminous binders used in road construction. The study utilized laboratory experiments and various analysis methods to investigate the fatigue resistance of different binders. The main objective was to develop a comprehensive evaluation that includes two distinct methods for analyzing fatigue and three different approaches for determining fatigue failure criteria.

The results of the study showed that the fatigue resistance of binders is strongly influenced by aging and polymer modification. The use of the linear amplitude sweep (LAS) test as the main protocol allowed for a faster estimation of fatigue resistance compared to traditional time sweep tests. Three failure criteria were analyzed: peak shear stress, 35% reduction in loss shear modulus, and pseudo strain energy.

The comparison of the three failure criteria revealed that the peak shear stress and pseudo strain energy criteria provided consistent results for most binders. However, the 35% reduction in loss shear modulus criterion showed underestimated results and highlighted the effect of aging in a way that was not expected. This criterion may not be suitable for comparing the effect of aging in analyzing LAS results.

The analysis also showed that the fatigue life of binders varies with strain level and aging condition. Aging had a detrimental effect on fatigue life at high strain levels, but a beneficial impact at low strain levels. The findings challenge the prevailing notion that aging leads to increased vulnerability to fatigue cracking in binders.

Furthermore, a comparison of the different failure criteria demonstrated the importance of considering multiple criteria to comprehensively evaluate the performance of asphalt binders. The results showed that the 35% reduction in  $|G^*| \cdot \sin \delta$  failure criterion provided more conservative estimates of fatigue life compared to the other criteria.

In addition to the findings related to failure criteria, this study also demonstrated the importance of considering polymer modification in evaluating the fatigue resistance of asphalt binders. The results showed that polymer modification can significantly improve the fatigue life of binders, especially at high strain levels. The use of polymer-modified binders can therefore be an effective strategy for enhancing the durability of road surfaces.

The study also highlights the need for more accurate and efficient methods for evaluating the fatigue resistance of asphalt binders. The LAS test used in this study showed promising results, but further research is needed to validate its effectiveness and reliability. The development of more advanced testing protocols and analysis methods can improve our understanding of the complex mechanisms underlying fatigue failure in asphalt mixtures.

Moreover, the findings of this study have implications for pavement design and maintenance practices. The use of binders with higher fatigue resistance can lead to longer lasting and more sustainable road surfaces. The results also suggest that aging can have a significant impact on the fatigue resistance of asphalt binders, highlighting the importance of proper storage and handling of binder samples to minimize aging effects.

Finally, this thesis contributes to the broader goal of improving the sustainability and resilience of road infrastructure. The findings can inform policy decisions related to road construction and maintenance, promoting the use of more durable and sustainable materials. By improving our understanding of the factors influencing fatigue failure in asphalt mixtures, we can develop more effective strategies for enhancing the durability and lifespan of road surfaces, ultimately leading to safer and more efficient transportation systems.

Overall, this investigation contributes to the understanding of fatigue properties of bituminous binders and provides insights for improving road infrastructure sustainability. The findings have important implications for pavement design and construction practices, highlighting the need for careful selection and evaluation of asphalt binders based on their fatigue resistance. Future research can further explore the relationship between binder properties, aging, and fatigue performance to enhance road durability and lifespan.

## References

- [1] Safaei, F. and Castorena, C., 2016. Temperature effects of linear amplitude sweep testing and analysis. *Transportation Research Record*, 2574(1), pp.92-100.
- [2] Kim, Y.R. and Little, D.N., 2004. Linear viscoelastic analysis of asphalt mastics. *Journal of Materials in Civil Engineering*, 16(2), pp.122-132.
- [3] Lytton, R.L., Uzan, J., Fernando, E.G., Roque, R., Hiltunen, D. and Stoffels, S.M., 1993. *Development and validation of performance prediction models and specifications for asphalt binders and paving mixes* (Vol. 357). Washington, DC: Strategic Highway Research Program.
- [4] Planche, J.P., Anderson, D.A., Gauthier, G., Le Hir, Y.M. and Martin, D., 2004. Evaluation of fatigue properties of bituminous binders. *Materials and Structures*, 37, pp.356-359.
- [5] Yang, K., Cui, H., Ma, X. and Zhu, M., 2023. Understanding and characterizing the fatigue cracking resistance of asphalt binder at intermediate temperature: A literature review. *Construction and Building Materials*, 407, p.133432.
- [6] -Lytton, R.L., Uzan, J., Fernando, E.G., Roque, R., Hiltunen, D. and Stoffels, S.M., 1993. *Development and validation of performance prediction models and specifications for asphalt binders and paving mixes* (Vol. 357). Washington, DC: Strategic Highway Research Program.
- [7] -Hajj, R. and Bhasin, A., 2018. The search for a measure of fatigue cracking in asphalt binders—a review of different approaches. *International Journal of Pavement Engineering*, 19(3), pp.205-219.
- [8] Anderson, D.A., Le Hir, Y.M., Marasteanu, M.O., Planche, J.P., Martin, D. and Gauthier, G., 2001. Evaluation of fatigue criteria for asphalt binders. *Transportation Research Record*, 1766(1), pp.48-56.

- [9] Zhang, H., Shen, K., Xu, G., Tong, J., Wang, R., Cai, D. and Chen, X., 2020. Fatigue resistance of aged asphalt binders: An investigation of different analytical methods in linear amplitude sweep test. *Construction and Building Materials*, 241, p.118099.
- [10] Sabouri, M., Mirzaiyan, D. and Moniri, A., 2018. Effectiveness of Linear Amplitude Sweep (LAS) asphalt binder test in predicting asphalt mixtures fatigue performance. *Construction and Building Materials*, 171, pp.281-290.
- [11] AASHTO (2018) Standard method of test for estimating fatigue resistance of asphalt binders using the linear amplitude sweep. AASHTO TP101-12, Washington, DC
- [12] Johnson, C.M., 2010. *Estimating asphalt binder fatigue resistance using an accelerated test method* (Doctoral dissertation).
- [13] Hintz, C., Velasquez, R., Johnson, C. and Bahia, H., 2011. Modification and validation of linear amplitude sweep test for binder fatigue specification. *Transportation Research Record*, 2207(1), pp.99-106.
- [14] AASHTO Standard T 391. (2020). Standard method of test for estimating fatigue resistance of asphalt binders using the linear amplitude sweep, American Association of State Highway and Transportation Officials, Washington, D.C., United States.
- [15] Hintz, C. and Bahia, H., 2013. Simplification of linear amplitude sweep test and specification parameter. *Transportation Research Record*, 2370(1), pp.10-16.
- [16] Daniel, Jo Sias, William Bisirri, and Y. Richard Kim. "Fatigue evaluation of asphalt mixtures using dissipated energy and viscoelastic continuum damage approaches (with discussion)." *Journal of the Association of Asphalt Paving Technologists* 73 (2004).
- [17] Safaei, F., Lee, J.S., Nascimento, L.A.H.D., Hintz, C. and Kim, Y.R., 2014. Implications of warm-mix asphalt on long-term oxidative ageing and fatigue performance of asphalt binders and mixtures. *Road Materials and Pavement Design*, 15(sup1), pp.45-61.
- [18] Miró, R., Martínez, A.H., Moreno-Navarro, F. and del Carmen Rubio-Gámez, M., 2015. Effect of ageing and temperature on the fatigue behaviour of bitumens. *Materials & Design*, 86, pp.129-137.

- [19] Shen, S., Airey, G.D., Carpenter, S.H. and Huang, H., 2006. A dissipated energy approach to fatigue evaluation. *Road materials and pavement design*, 7(1), pp.47-69
- [20] Sabouri, M. and Kim, Y.R., 2014. Development of a failure criterion for asphalt mixtures under different modes of fatigue loading. *Transportation Research Record*, 2447(1), pp.117-125.
- [21] Chen, H., Zhang, Y. and Bahia, H.U., 2021. Estimating asphalt binder fatigue at multiple temperatures using a simplified pseudo-strain energy analysis approach in the LAS test. *Construction and Building Materials*, 266, p.120911.
- [22] AASHTO Provisional Standard TP 101-12. (2012). Standard method of test for estimating fatigue resistance of asphalt binders using the linear amplitude sweep, American Association of State Highway and Transportation Officials, Washington, D.C., United States.
- [23] Wang, C., Castorena, C., Zhang, J. and Richard Kim, Y., 2015. Unified failure criterion for asphalt binder under cyclic fatigue loading. *Road Materials and Pavement Design*, 16(sup2), pp.125-148.
- [24] AASHTO T 391-20. *Estimating fatigue resistance of asphalt binders using the linear amplitude sweep*. American Association of State Highway and Transportation Officials, 2020.
- [25] AASHTO Provisional Standard TP 101-14. (2014). Standard method of test for estimating damage tolerance of asphalt binders using the linear amplitude sweep, American Association of State Highway and Transportation Officials, Washington, D.C., United States.
- [26] Safaei, F., Castorena, C. and Kim, Y.R., 2016. Linking asphalt binder fatigue to asphalt mixture fatigue performance using viscoelastic continuum damage modeling. *Mechanics of Time-Dependent Materials*, 20, pp.299-323.
- [27] Hofko, B. and Hospodka, M., 2016. Rolling thin film oven test and pressure aging vessel conditioning parameters: Effect on viscoelastic behavior and binder performance grade. *Transportation Research Record*, 2574(1), pp.111-116.
- [28] Migliori, F. and Corté, J.F., 1998. Comparative study of RTFOT and PAV aging simulation laboratory tests. *Transportation research record*, 1638(1), pp.56-63.

- [29] Aashto, R., 2009. Standard practice for accelerated aging of asphalt binder using a pressurized aging vessel (PAV). *American Association of State Highway Transportation Officials*.
- [30] Anderson, D. A., & Bonaquist, R. F. (2012). *Investigation of Short-term Laboratory Aging of Neat and Modified Asphalt Binders*. Transportation Research Board.
- [31] Bahia, H.U. and Anderson, D.A., 1995. The Pressure Aging Vessel (PAV): a test to simulate rheological changes due to field aging. *ASTM special technical publication, 1241*, pp.67-88.
- [32] Kanabar, A., 2012. *Physical and chemical aging behavior of asphalt cements from two northern Ontario pavement trials*. Library and Archives Canada= Bibliothèque et Archives Canada, Ottawa.
- [33] Farrar, M., Sui, C., Salmans, S. and Qin, Q., 2015. Determining the low-temperature rheological properties of asphalt binder using a dynamic shear rheometer (DSR). *Report 4FP, 8*, p.20.
- [34] Jia, J. and Zhang, X.N., 2005. Modification of the rolling thin film oven test for modified asphalt. *SATC 2005*.
- [35] Santagata, M., Dalmazzo, D. and Santagata, E., 2008. Deformation behavior of clay-water suspensions from rheological tests. In *Proc., 4th Int. Symp. Deformation Characteristics of Geomaterials* (Vol. 1, pp. 453-459).
- [36] Test, O., 2010. Determining the rheological properties of asphalt binder using a dynamic shear rheometer (DSR). *Washington, DC*.
- [37] Schapery, R.A., 1984. Correspondence principles and a generalized J integral for large deformation and fracture analysis of viscoelastic media. *International journal of fracture, 25*, pp.195-223.
- [38] Saboo, N., 2020. New damage parameter for fatigue analysis of asphalt binders in linear amplitude sweep test. *Journal of Materials in Civil Engineering, 32(6)*, p.04020126.
- [39] Wang, Y. and Richard Kim, Y., 2019. Development of a pseudo strain energy-based fatigue failure criterion for asphalt mixtures. *International Journal of Pavement Engineering, 20(10)*, pp.1182-1192.